HHS Public Access

Author manuscript

Annu Rev Phys Chem. Author manuscript; available in PMC 2024 July 11.

Published in final edited form as:

Annu Rev Phys Chem. 2011 ; 62: 437–463. doi:10.1146/annurev-physchem-032210-103526.

Toward a Molecular Theory of Early and Late Events in Monomer to Amyloid Fibril Formation

John E. Straub[1], **D. Thirumalai**[2]

[1]Department of Chemistry, Boston University, Boston, Massachusetts 02215

[2]Biophysics Program, Institute for Physical Science and Technology, and Department of Chemistry and Biochemistry, University of Maryland, College Park, Maryland 20742

Abstract

Quantitative understanding of the kinetics of fibril formation and the molecular mechanism of transition from monomers to fibrils is needed to obtain insights into the growth of amyloid fibrils and more generally self-assembly multisubunit protein complexes. Significant advances using computations of protein aggregation in a number of systems have established generic and sequence-specific aspects of the early steps in oligomer formation. Theoretical considerations, which view oligomer and fibril growth as diffusion in a complex energy landscape, and computational studies, involving minimal lattice and coarse-grained models, have revealed general principles governing the transition from monomeric protein to ordered fibrillar aggregates. Detailed atomistic calculations have explored the early stages of the protein aggregation pathway for a number of amyloidogenic proteins, most notably amyloid β – (Aβ –). protein and fragments from proteins linked to various diseases. These computational studies have provided insights into the role of sequence, role of water, and specific interatomic interactions underlying the thermodynamics and dynamics of elementary kinetic steps in the aggregation pathway. Novel methods are beginning to illustrate the structural basis for the production of Aβ-peptides through interactions with secretases in the presence of membranes. We show that a variety of theoretical approaches, ranging from scaling arguments to minimal models to atomistic simulations, are needed as a complement to experimental studies probing the principles governing protein aggregation.

Keywords

amyloid disease; amyloid β-protein; kinetics of fibril growth; aggregation mechanism; coarse-grained models

straub@bu.edu .

DISCLOSURE STATEMENT

The authors are not aware of any affiliations, memberships, funding, or financial holdings that might be perceived as affecting the objectivity of this review.

1. INTRODUCTION

Almost all proteins and even very short peptides, which have little to no sequence identity, can form amyloid fibrils in vitro under appropriate conditions (such as temperature, pH, presence of ions and cosolvents) (1, 2). Surprisingly, it has been found that amyloid fibrils formed from nondisease-related proteins can be neurotoxic (3, 4). Understanding the factors that contribute to the growth kinetics of oligomers and amyloid fibrils should lead to methods that can be used to prevent or control their formation. Although much attention has focused on the link between amyloids and various diseases, recent studies have also pointed out potential benefits (5). Interestingly and regardless of the functional roles, it is suspected that amyloid fibrils adopt a characteristic cross β-structure independent of sequences or the specific monomer structures. These observations raise a number of fundamental questions pertaining to the energetics and kinetics of amyloid formation, the resolution of which is necessary to obtain insights into the steps leading to their formation and ultimately their biological functions.

Recent reports suggest that there may be similarities in the assembly mechanism of amyloidogenic peptides and proteins as well (6–8). Indeed, the behavior of many of these proteins, including prion protein PrP^C, may be so similar that fibrillar states of Aβ-peptides can themselves serve as a pathogenic agent, much like the scrapie form of PrP^C does as implied by the protein-only hypothesis (9). These findings suggest that the growth mechanism of all amyloidogenic proteins (including α-synuclein, Aβ-peptides, and PrP^C) may share essential characteristics. As such, it is important to explore and provide an understanding of the kinetics and thermodynamics underlying the cascade of steps in the assembly of monomeric protein into oligomers and ultimately fibrils.

Given the complexity of in vivo and in vitro amyloid fibril formation, it is not surprising that a range of methods has been brought to bear to describe the link between structure, aggregation kinetics, and function (10, 11). In this context, theory and computations have played increasingly important roles in elucidating the salient biophysical aspects of amyloid formation. The ultimate goal motivating many computational and theoretical studies is to extract unifying principles governing protein aggregation using detailed studies of a large number of models (12).

In recognition of the universal features observed in fibril formation, it is appreciated that studies on amyloidogenic peptides may provide fundamental insights into the behavior of proteins that display similar aggregation propensities. Moreover, many critical observations regarding the energetics and kinetics of these systems have been derived from experiments on amyloidogenic peptide fragments. The availability of high-resolution structures of several amyloid peptide fragments (13) has made it possible to address a number of biophysical questions in a nearly quantitative manner (14).

In this article, we provide perspectives on the molecular basis of the sequence-dependent properties of protein aggregation by building on recent theoretical studies that have explored fundamental aspects of the thermodynamics and kinetics of peptide association in important amyloid proteins. We discuss key questions related to the nature and relevance of

mechanisms and the associated timescale for amyloid formation, from oligomers to fibrils, and provide concise views of theoretical and computational approaches that have provided insights into fundamental aspects of the amyloid aggregation. The principles that govern fibril formation are likely to be applicable to a range of problems associated with self-assembly of large molecular complexes. Functions of many enzymes, virus assembly, and molecular machines are carried out by proteins with multiple domains. Their self-assembly is driven also by mechanisms that are not dissimilar from those involved in amyloid-fibril formation. For these reasons, it is important to develop a unified perspective of the factors that determine how multisubunit proteins assemble.

2. GENERAL ASPECTS OF PROTEIN AGGREGATION MECHANISM AND FIBRIL GROWTH

From experimental and computational studies of amylogenesis, several distinct scenarios for fibril formation and elongation have emerged (10, 15–17). In one scenario, largely unstructured peptide monomers in solution cluster and form nuclei (10). When the cluster reaches a critical nucleus, that nucleus then grows to form full-length fibrils by the addition of monomers to the existing fibril ends (18, 19). Essentially similar mechanisms, describing the overall aggregation process in terms of elementary kinetic steps, have been developed in greater detail (20–23). There has been a coordinated effort to use experimental data to assign values to the elementary rate constants, to identify the size of the critical nucleus, and to understand how the overall kinetic network may be influenced by the presence of cofactors (24–28) and secondary processes (29).

In a second scenario, there is first the formation of peptide protofibrils of intermediate length (30, 31). Such protofibrils then associate to form full-length fibrils (31, 32). Once full-length fibrils are formed, the amyloid peptide may add directly to existing fibrils or protofibrils (21, 33). Finally, monomers may associate to form micelles, which may convert to fibril nuclei upon reaching a critical size (10, 18, 19). The relative importance of these possible pathways has not been clearly established for any aggregating protein.

Regardless of how the fibrils are initially formed, it has been demonstrated that the process of fibril elongation occurs through the process of monomeric peptide binding to fibril ends (33). The key observation that the kinetics appears to be first order in the concentration of monomeric peptide has motivated further studies of the kinetics of fibril elongation (21, 31). Analysis of the elongation rate constant has led to the development of an energy-landscape theory of amyloid peptide fibril elongation (34). The energy-landscape perspective not only articulates distinct scenarios for protein aggregation (17), but also has led to quantitative models for fibril formation (34). Recently, there has been renewed interest in the development of more detailed rate theories that explore how the elementary steps in fibril elongation may be understood in terms of characteristics of the underlying energy landscape (35, 36).

2.1. Generic Fibril Growth Mechanism

Over 10 years ago, we proposed a simple set of elementary kinetic steps that capture the essential peptide dynamics of first-order fibril growth (34). This model can be interpreted graphically in terms of diffusive dynamics on the amyloid peptide energy landscape depicted in Figure 1. The complex fibril-formation kinetics indicates that at each step of protein association there are pathway bifurcations leading to population of a spectrum of species. This implies that the energy landscape for protein aggregation is rugged. Nevertheless, from the simplified representation in Figure 1, we deduce that the height of the landscape is a measure of the free energy of the monomer fibril system as a function of (*a*) the separation between the peptide monomer and the existing fibril and (*b*) a coordinate that measures the conformation of the peptide monomer/fibril as it undergoes a transition between the collapsed-coil conformation and the β form favored in the fibril.

In the two-step dock-and-lock mechanism (37), the partially structured collapsed-coil state docks with the fibril end through diffusion-limited kinetics. The peptide/fibril complex then undergoes reorganization to accommodate and lock the peptide in a deposited product state. The reorganization step may involve conformational changes in the peptide and/or the fibril end so that on completion of the lock step, the peptide adopts a structure that is commensurate with the underlying fibril. At higher concentrations, at which the timescale of peptide reorganization and locking exceeds that of diffusional encounter, the barrier for peptide reorganization may increase as a function of the local peptide concentration. The activation energy for the fibril elongation is associated with peptide/fibril reorganization.

Alternatively, in a one-step mechanism the monomeric peptide undergoes a conformational fluctuation into an aggregation-prone state (Figure 1). When the timescale for the diffusional encounter with the fibril is short compared with the lifetime of the aggregation-prone state, the peptide will encounter and deposit on the fibril end with an inconsequential time required for reorganization (34). The activation energy is associated with the peptide monomer reorganization in solution from a set of unreactive configurations to one of a set of transition-state configurations.

The general aspects of this model capture the essential features of kinetic data for fibril elongation (17, 34). Subsequent simulation studies employing minimal coarse-grained models of protein aggregation have both confirmed the validity of our model and provided insights into the role of the relative probability of the N^* aggregation-prone conformers of the monomeric protein, energetics of interpeptide interactions that stabilize the growing aggregate, and the diversity of protein conformational ensembles observed in aggregation and fibril formation (38–45).

In particular, the model of Pellarin & Caflisch (43), which used an internal potential to bias peptide configurations toward amyloid-competent (aggregation-prone) states (46), elucidates many aspects of the scenarios that emerge from a global energy-landscape perspective (34). By enhancing the bias toward aggregation-prone states, they could observe a transition from disordered aggregation (weak bias toward N^*), to ordered fibril formation with on-pathway intermediates (moderate bias of N^*), to ordered fibril formation without intermediates (strong bias of N^*). In terms of the energy-landscape model, this can be seen as a transition

between the two-step dock-and-lock mechanism and the one-step model of fast deposition (34). In addition, the coarse-grained model simulations provide insight into the nature of the lag phase preceding fibril formation, the correlation between mechanism and the degree of internal bias of the N^* states, and a detailed structural analysis of the aggregation state network (46). Similar qualitative features were observed and validated by Bellesia & Shea (45, 47, 48) in subsequent studies using a more complex coarse-grained model.

2.2. Rate Theory for Elementary Steps in the Aggregation Process

The qualitative features of fibril growth kinetics gleaned from the energy-landscape picture (17) can be made more precise using diffusion-limited aggregation kinetics (34). The Smoluchowski rate theory readily provides an estimate of the equilibrium flux for the formation of contact between two species P and m of radii σ_P and σ_m diffusing in solution with a relative diffusion coefficient $D = D_P + D_m$. The association rate constant is

$$k_a^D = 4\pi D(c)\sigma\alpha, \tag{1}$$

where $\sigma = \sigma_P + \sigma_m$ is the contact radius, α is a measure of the probability that on contact the peptide deposits on the fibril, and we have indicated that the diffusion coefficient $D(c) = k_B T/\eta(c)$ is expected to be a function of the monomeric peptide concentration c through the specific viscosity $\eta(c)$. We assume that the fibril is sufficiently large so that growth occurs by diffusional encounter of fluctuating monomers with a stationary amyloid fibril.

The overall solution concentration can be written as a sum of the pure solvent viscosity, η_0, and the specific viscosity contribution due to the presence of the protein, η_c. The concentration dependency of the overall solution viscosity can be written as

$$\eta(c) = \eta_0 + \eta_c c + k_H \eta_c^2 c^2 + \cdots, \tag{2}$$

where k_H is the Huggins coefficient, which captures the effect on the solvent viscosity due to protein-protein interactions (49). The overall association rate may then be written as

$$k_a^D \approx \frac{4\pi k_B T \sigma \alpha}{\eta_0 + \eta_c c + k_H \eta_c^2 c^2}. \tag{3}$$

The expression in Equation 3 predicts a turnover in the overall reactive flux, $k_a^D c$, as a function of monomer concentration c. (*a*) In the limit of infinite dilution ($c \to 0$), the expression reduces to the simple Smoluchowski limit and is independent of c (34). The overall reaction flux is proportional to the monomeric protein concentration at low c. (*b*) In the limit of low but finite protein concentration, $\eta_0/\eta_c < c$, the solution viscosity will vary as

first order in c, and the reaction flux will vary in proportion to $c/(1 + (\eta_c/\eta_0)c)$, similar in form to a recently proposed result based on more detailed arguments (35). (*c*) In the interesting limit of higher monomeric protein concentration, $1/(k_H\eta_c) < c$, the reactive flux is predicted to vary inversely with the protein concentration and the Huggins coefficient, indicating the important role of protein-protein interactions in modulating the rate of aggregation at higher c.

It has been shown that the monomer of the amyloid peptide congener in aqueous solution has a large hydrophobic surface area (50). More detailed kinetic models of aggregation kinetics, focusing on the essential role of hydrophobic interactions in stabilizing the growing protein aggregates (51), are consistent with this point of view and have led to more detailed estimates regarding the size of the critical nucleus in the early stages of the aggregation pathway (52).

In many cases, the formation of a contact is not enough for a reaction to occur. It is also necessary for the protein in contact to overcome an activation energy barrier to form product. If the activation barrier is $G_a^\dagger$, then the Debye-Smoluchowski rate constant for reaction is simply the rate of forming a contact multiplied by the probability of the reactant being activated at the time the contact is formed or

$$k_a^{DS} = 4\pi D(c)\sigma\alpha \ \exp\left(-G_a^\dagger/RT\right). \tag{4}$$

Precise experiments over a range of c can be used to extract α (Equation 1) and $G_a^\dagger$ (Equation 4).

3. UNIVERSAL NATURE OF AGGREGATION-PRONE STATES AND THE MOLECULAR BASIS FOR PROTEIN AGGREGATION

Typically, monomers of proteins and peptides that aggregate are either unstructured (such as α-synuclein and Aβ-peptides) or folded (such as TTR and PrP^C). This has led to the suggestion that fibril formation requires partial unfolding of the native structure (53, 54) or partial folding of natively unstructured proteins (17) to populate the aggregation-prone state N^* (see Figure 2).

Transthyretin is an example of a protein that requires partial unfolding of the native state to populate N^* (55). In contrast, it was shown first by computations (56, 57) and subsequently in experiments (58) that N^* in prions is more stable than the cellular form. However, a large free energy barrier between PrP^C and N^* prevents formation of the latter during the normal turnover of the protein (17). Because $A\beta$-peptides and human amylin are often assumed to have substantial random-coil character in the monomeric states, the initial aggregation is presumed to occur by partial folding of the unfolded state (59). Regardless of whether the monomer is structured, it is clear that for aggregation to occur fluctuations, due to thermal or denaturation stress, have to populate the N^* conformation.

Three conclusions can be drawn from these observations: (*a*) Sequences and/or environmental factors that promote the N^* state would result in an enhanced tendency to aggregate. (*b*) Because conformations of the N^* state, a non-native structure, constitute an ensemble, it is reasonable to ask whether the morphology of the fibril reflects the precise structure of the monomer that nucleates to the fibril state. It follows that, to fully describe aggregation and growth, it is crucial to understand how protein sequence and external conditions modulate the production of N^*. (*c*) The N^* structures should be viewed as an ensemble. Different members in the ensemble can associate to form fibrils with varying morphologies giving rise to fibril polymorphism. According to this picture, the seeds to polymorphism may be encoded in the spectrum of N^* structures in the monomer.

These considerations demonstrate that the molecular basis for describing aggregation, which is likely to contribute to the design of small-molecule drugs that can inhibit a given kinetic step, will require a quantitative description of the dynamics involved in the cascade of events that drive the transition from monomer to fibril. This daunting task requires careful experimental studies as well as multifaceted computational approaches (12, 17, 60, 61).

3.1. Link Between Spectrum of Conformational States of Monomers and Fibril Formation

To follow the events that drive the transition between monomers and fibrils, researchers constructed a lattice model for aggregation (62). The use of lattice models has been criticized for sacrificing details, which are no doubt important in characterizing the stability of amyloid fibrils. Nevertheless, lattice models have yielded great insights into problems related to protein folding, protein evolution, and protein aggregation (63–66). Moreover, a significant appeal of simple lattice models is the ability to precisely evaluate simulation results without concerns regarding incomplete configurational sampling or broken ergodicity that are ever present when analyzing simulations of protein aggregation employing all-atom models (67–69).

A principal focus in constructing these lattice models was to test an important hypothesis that the structure adopted by the monomer in the fibril must be similar to a high free energy state in the monomer. To develop this hypothesis, investigators modeled each polypeptide chain as having N connected beads that are confined to the vertices of a cube (62). The simulations were performed using M identical chains with $N = 8$. The sequence of a chain is +HHPPHH−, where + and − are charged beads and H and P model hydrophobic and hydrophilic sites, where HH contacts are stabilizing (see Figure 3). The advantage of a small system is all conformations that the monomer can adopt (1,831 in all), and the associated energies can be enumerated. This allows for the exact computation of the partition function. Simulations were performed at low-enough temperatures that the isolated monomer adopts a stable compact native conformation.

Exact enumeration of all possible conformations of the monomer of eight beads demonstrated that there are 18 energy levels. Three of them are shown in Figure 3. The monomeric native state is compact and has the lowest energy ($E = -3.8$). It should be noted that the conformation of the chain in the fibril state is not compact and belongs to the first excited state (label N^* in Figure 3a), which is fourfold degenerate.

Fluctuations in the monomer conformation must populate the structure with $E = -3.4$ to initiate oligomerization. Under conditions in which the native structure is stable, such fluctuations can occur spontaneously or through interchain interactions. Clearly, suppression of fluctuations at low temperatures would slow the process of oligomerization (53). The toy model clearly illustrates the well-accepted proposition that aggregation requires partial unfolding of the native conformation. The results for this exactly soluble model show that analysis of the free energy spectrum of the monomer provides clues as to the structures that can form fibrils, thus validating the hypothesis.

3.2. Probing the Mechanisms of Fibril Formation Using Lattice Models

The kinetics and mechanism of fibril formation using lattice models and exhaustive MC simulations have been studied as a function of temperature (T) and the number of chains (M) (62). A number of generic features thought to govern fibril assembly were captured by this toy model. The monomer, which contains eight beads made from three types of letters (hydrophobic, polar, and charged), adopts a compact conformation in the native state. In both the single-layer protofilament (seen for $M \leq 10$) and the two-layer fibril ($M \geq 10$) structures, the monomers are arranged in an antiparallel fashion with a strand-like conformation that is perpendicular to the fibril axis. The contacts in the N^* conformation, which is one of four structures in the first excited state of the monomer, are also present in the native conformation. The timescale for fibril formation is a minimum in the T range when the N^* conformation is substantially populated (Figure 3b).

The results of these simulations suggest that fibril assembly occurs in three distinct stages. In each stage there is a cascade of events that transforms the monomers and oligomers to ordered structures (Figure 3c). In the first burst stage, highly mobile oligomers of varying sizes form. The conversion to the N^* conformation occurs within the oligomers during the second stage, in which a vast number of interchain contacts are established. As time progresses, a dominant cluster emerges that contains a majority of the chains. In the final stage, the aggregation of N^* particles serves as a template onto which smaller oligomers or monomers can dock and undergo conversion to fibril structures.

The detailed analysis shows that elements of the three popular models for fibril formation, namely nucleation and growth, templated assembly, and nucleated conformational conversion, are present at various stages of fibril assembly (62, 70).

4. MONOMER ADDITION TO GROWING A β-PROTEIN OLIGOMERS BY A DOCK-AND-LOCK MECHANISM

According to the amyloid hypothesis (71), Alzheimer's disease (AD) is caused by the accumulation of the Aβ-peptide, which is a normal byproduct of the metabolism of amyloid precursor protein (APP), which occurs throughout life (72–76). Single-site mutations in the Aβ-protein sequence have been correlated with variable AD pathology shown to demonstrate significant variations in fibril growth rates (34, 77–79). Recognizing the importance of oligomer formation in amyloidogenic diseases, an examination of the energetics and dynamics of this process as well as characterization of the pathogenic properties of amyloid

protein oligomers has become a principal focus of research. It is important to understand the factors that contribute to the thermodynamics and kinetics of oligomer formation, which is an essential step in the cascade of events that turn the disordered collapsed-coil form of Aβ-peptide monomers into fibrils typified by a cross β-structure.

One of the most significant challenges in understanding amyloid formation is to describe in molecular detail the cascade of structural transitions that occur as monomers collide to form oligomers and subsequently grow to form fibrils. It is difficult to characterize experimentally the structural transitions that occur in the early stages of fibril formation because of the large conformational fluctuations associated with soluble oligomers. Given the suspicion that the oligomers of amyloidogenic peptides are themselves toxic, it is crucial to understand how they form from monomers (80).

4.1. Kinetic Basis of the Dock-Lock Growth Mechanism of Amyloid Fibrils

To probe the dynamics of oligomer growth, researchers investigated the assembly mechanism

$$[A\beta_{16-22}]_{(n-1)} + A\beta_{16-22} \rightleftharpoons [A\beta_{16-22}]_n$$

using extensive molecular dynamics simulations in explicit water (81). By monitoring the evolution of the β-strand content in each of the peptides as a function of time, they analyzed the mechanism of association of a monomeric strand with the preformed oligomer and its eventual addition to the growing aggregate. The unstructured monomer was found to add to the structured oligomer by a two-phase dock-lock mechanism that is strikingly similar to that proposed for fibril growth (37). In the first rapid dock phase, the unstructured $A\beta_{16-22}$ docks onto a preformed oligomer. In the second lock phase, interaction of the monomer with the fluid-like template results in substantial conformational changes. In the lock phase, the preformed oligomer itself dynamically fluctuates to accommodate the monomer. The two-step addition, which is a simplification of a more complex dynamics, has also been confirmed in subsequent studies (82). More recently, a thermodynamic perspective of the complex growth process has been provided (82, 83) and further analyzed in terms of specific side-chain interactions in Aβ-peptide (84).

We now consider the special case of the reaction $(A\beta_{16-22})_5 + A\beta_{16-22} \Rightarrow (A\beta_{16-22})_6$. In the absence of interaction with the oligomer, the probability of being in the β-strand conformation was computed to be approximately 0.1. The monomer is in a relatively compact state, whereas interaction with the oligomer leads to an extension of the chain and an increase in the β-strand content, which was monitored using $\beta(t)$, the instantaneous strand content of the monomer or the oligomer. Figure 4 shows that the high initial β-strand content of the oligomer is maintained during the course of the simulation. The β-strand content of the added monomer grows in stages. In the first phase, the β-strand content increases substantially from its initial value. The inset shows that most of the growth occurs immediately upon docking. Within 1 ns after interaction with the pentamer, the β-strand content of the added monomer was observed to increase to approximately 0.3. The extent of strand formation continues to increase over a period of tens of nanoseconds and fluctuates

around 0.65 for approximately 100 ns. During the initial docking stage there are large changes in the structure of the nascent monomer. Given that the monomer is a small peptide, there is a relatively sharp transition, which defines the locking stage, in which the β-strand content of the added monomer approaches that of the preformed pentamer. In this trajectory the average β-strand content of the peptides in the pentamer fluctuates around 0.8, and the resulting oligomer is reminiscent of a fluctuating nematic droplet.

4.2. Search for a Critical Nucleus in the Transition from Oligomers to Fibrils

To identify the size of a critical nucleus for oligomer growth, researchers explored the reaction for $n = 4, 5$, and 6 and concluded that the time needed to incorporate the monomer into the fluid-like oligomer grows even when $n = 6$, which suggests that the critical nucleus size must exceed 6. Stable antiparallel structure formation exceeds hundreds of nanoseconds even though frequent interpeptide collisions occur at elevated monomer concentrations used in the simulations.

The simulation results suggest that the timescale for the lock stage is considerably longer than for the dock phase. The large separation in the rates of the dock and lock phases is consistent with experimental findings that have probed the kinetics of monomer addition to the ends of a fibril (37, 85). It appears that in the growth of the fibrils and prenucleus oligomers the rate-limiting step is the locking phase. The rate-determining step in the monomer addition is the lock phase in which both the preformed oligomer and the monomer undergo combined conformational changes that form a stable antiparallel higher-order oligomer. Because the biophysical basis of the oligomer assembly mechanism is general, it has been proposed that the growth of other amyloidogenic peptides might also follow the dock-lock mechanism. Testing this conjecture on alternative fragments of the Aβ-protein as well as other amyloidogenic peptides is an important goal for future studies.

5. EXPLORING ATOMIC-LEVEL CHARACTERISTICS OF THE AGGREGATION-PRONE SPECIES OF Aβ-PROTEIN

Exploration of the nature of the protein aggregation pathway suggests that there are common characteristics of the fibril-formation mechanism that may prove to be independent of the specific protein sequence. One such unifying aspect, suggested by computational studies of coarse-grained simulations of protein aggregation using on- and off-lattice models, is the essential role of the aggregation-prone N^* state. It is reasonable to expect that sequences and/or environmental factors that stabilize the aggregation-prone N^* state enhance aggregation. It is further possible that the morphology of the resulting fibril may reflect the precise structure of the aggregation-protein monomer that nucleates formation of the fibril state.

The nature of putative aggregation-prone states has been studied most extensively for the case of the Aβ-protein and its congener peptides. We summarize a number of studies that have provided insight into the ensemble of structures composing the Aβ-protein ensemble and the structure and stability of putative aggregation-prone species within the larger amyloid protein ensemble. These studies provide support for the essential role of

aggregation-prone states in the overall amyloid aggregation pathway and suggest how the role of sequence and environmental effects can be used to explore the subtle variations in the stability of those species that can critically influence the overall rate of protein aggregation.

5.1. Expulsion of Discrete Waters Facilitates Formation of Stabilizing Contacts in the Early Stages of Oligomer Formation

In the amyloid fibrils formed from long fragments of the Aβ-protein, the monomers are in parallel arrangement and lie perpendicular to the fibril axis (86, 87). The structure of the monomers satisfies the amyloid self-organization principle—the low free energy state of the monomer maximizes the number of intra- and interpeptide contacts and salt bridges (88). For Aβ_{10-35} the principle suggests that the formation of the intramolecular salt bridge between Asp23-Lys28 (D23-K28) ensures that unpaired charges are not buried in the low dielectric interior.

Using all-atom molecular dynamics simulations in explicit water, investigators explored the question of whether the D23-K28 interaction forms spontaneously in the isolated Aβ_{10-35} monomer (89, 90). To validate the simulation protocol, they demonstrated, using five independent trajectories spanning a total of 100 ns, that the pK_a values of the titratable groups are in good agreement with experimental measurements (89). The computed free energy disconnectivity graph shows that the ensemble of compact random-coil conformations can be clustered into four basins that are separated by free energy barriers ranging from 0.3 kcal mol^{-1} to 2.7 kcal mol^{-1} (Figure 5). The disrupted salt bridge is the more favorable state, and a large barrier makes the transition between the formed and disrupted substates improbable. Burying K28 in the peptide interior is an unfavorable process.

Owing to the desolvation penalty, the structural motif with a stable turn involving the residues $V^{24}GSN^{27}$ and a preformed D23-K28 contact is a minor component of the simulated structures. The extent of solvation of the peptide in the four basins varies greatly, which underscores the dynamical fluctuations in the monomer. These results suggest that expulsion of discrete water molecules (*a*) facilitates formation of the intramolecular D23-K28 salt bridge, (*b*) is apparently driven by interpeptide interactions, and (*c*) must be an early event in the oligomerization process.

5.2. Interactions Stabilizing N^* Structures Balance Sequence-Dependent Intrapeptide Electrostatic and Hydrophobic Interactions

The initial event in protein aggregation is driven by fluctuations that populate monomer conformations that are aggregation prone. These highly populated structures, driven by a balance between hydrophobic and electrostatic interactions in the protease-resistant Aβ_{21-30} peptide (91, 92), were analyzed using molecular dynamics simulations (93).

Analysis of the pK_a values of the titratable residues is consistent with the observation that E22 and D23 side chains infrequently form salt bridges with the K28 side chain. Structural analysis shows that the E22-K28 contacts are more probable in dried salt bridges, whereas D23-K28 contacts are more probable in solvated salt bridges. The populations of

the intrapeptide hydrophobic interactions increase as D23N < wild type (WT) < E22Q < K28A. Increased contacts of the K28 ammonium group with backbone oxygen atoms were observed in the WT and E22Q peptides when compared with the D23N peptide. Intrapeptide electrostatic interactions were connected to calculated pK_a values that compare well with the experimental estimates.

The influence of the titratable residues on the stability of V^{24} GSN^{27} was dissected using E22Q (Dutch), D23N (Iowa), and K28N mutants. Three hyperbasins are observed in the C_α(V24)-C_α(N27) versus SC(V24)-SC(K28) projection of the free energy. Basin I is characterized by a compact structure of the $V^{24}GSN^{27}$ segment of the $A\beta_{21-30}$ peptide. The peptide structures in basin II are described by strong hydrophobic interaction between the V24 and K28 side chains. The hydrophobic interactions cluster the $A\beta_{21-30}$ peptide into two basins, differentiated by the relative position of the $D^{23}VG^{25}$ and $G^{25}SN^{27}$ fragments about the G25 residue. The E22Q mutation increases the population of structures with an intact VGSN turn, which is proposed to be an essential structural motif in the aggregation of $A\beta$-peptide (50, 94, 95).

The increase in the population of structures in the aggregation-prone basin I in E22Q, which occurs solely because of the difference in charge states between the Dutch mutant and the WT, gives a structural explanation of the larger aggregation rate in the mutant (96). The D23N mutation dramatically reduces the intrapeptide interactions. The K28A mutation increases the intrapeptide hydrophobic interactions, which promotes the population of structures in basin I and basin II, characterized by hydrophobic interaction between the V24 and K28 side chains, with well-separated ends of the backbone atoms in the $V^{24}GSN^{27}$ turn. These results support the conjecture that mutations or sequences that enhance the probability of assembly-competent N^* conformations in basin I promote the aggregation of $A\beta$-peptides.

5.3. Covalent Constraints Stabilizing Aggregation-Prone Conformations of $A\beta$-Peptides Enhance the Rate of Fibril Formation

Recent experiments have shown that the $A\beta$-protein congener $A\beta_{1-40}$[D23 – K28], in which the side chains of residues Asp23 and Lys28 are linked by a lactam bridge, forms amyloid fibrils that are structurally similar to the WT $A\beta$-peptide at a rate that is nearly 1,000 times faster than the WT (97). All-atom molecular dynamics simulations of the WT dimer were used, as well as a monomer and dimers of $A\beta_{10-35}$[D23 – K28] with a constrained D23-K28 salt bridge in explicit solvent, to understand the origin of the observed enhanced rate of fibril formation (98). The simulations demonstrate that the assembly-competent monomers (N^*), with strand conformations in the residues spanning the N and C termini and a bend involving residues $D^{23}VGSNKG^{29}$, are populated to a greater extent in $A\beta_{10-35}$[D23 – K28] than in the WT, which has negligible probability of forming N^*.

The salt bridge in N^*, whose topology is similar to that found in the fibril, is hydrated. The reduction in the free energy barrier to fibril formation in $A\beta_{10-35}$[D23 – K28] compared with the WT is attributed to entropic restrictions that arise from the salt-bridge constraint. A decrease in the entropy of the unfolded state and the lesser penalty for conformational

rearrangement, including the formation of the salt bridge in Aβ-peptides with D23-K28 constrained, result in a reduction in the kinetic barrier in the constrained $A\beta_{1-40}[D23-K28]$ compared with the WT peptide.

Although a number of factors determine the growth of fibrils, the decrease in the free energy barrier of formation of N^* in the $A\beta_{1-40}[D23-K28]$ congener, relative to the WT peptide, is a major factor in the rate enhancement for fibril formation (97). Qualitatively similar results were obtained using simulations of $A\beta_{9-40}$ peptides. These results support the hypothesis that mutations or other constraints that preferentially enhance the population of N^* species enhance the rate of aggregation.

5.4. Role of Water in the Late Stages of Fibril Growth

The precise role of water in facilitating fibril growth is poorly understood. In a recent molecular dynamics simulation in explicit water, the process of monomer addition onto a preformed fibril was investigated (14). Assuming that the growth of fibrils occurs by the addition of one monomer at a time (34), the authors examined in detail the molecular conformational changes that occur after the monomer docks to one end of the fibril.

The fibril structure from the heptapeptide $G^1NNQQNY^7$ in the yeast prion Sup35 was chosen to elucidate the general scenarios for the addition of monomers (13). The acquisition of structure in the growth process was monitored by observing the increase in the β-strand content of the added monomer as a function of time. In the fibril structure, the residues N^3QQN^6 are in β-strand conformations. The equilibrium strand content for the four internal residues (N^3QQN^6) is defined as β_E in terms of the appropriate geometry for a β-strand.

The β-strand content as a function of time, $\beta(t)$, was calculated in steps of $\Delta = 1$ ns to probe the dynamics of changes in the monomer as it locks onto the fibril. If the locking process is complete, one expects that at long times the strand content of the monomer $\beta(t) \rightarrow \beta_E$. Remarkably, $\beta(t)$ of the initial unstructured monomer changes dramatically and highly cooperatively when $G^1NNQQNY^7$ locks onto the fibril (Figure 6c) in all three trajectories. Analysis of the time dependency of $\beta(t)$ shows that the strand content of the locking monomer reaches 0.25 rapidly and remains at this level for a duration ranging from 30 to 425 ns depending on the trajectory (Figure 6c). The transition time, Δt, in which $\beta(t)$ increases from 0.25 to 1.0 (Figure 6a), is much shorter than the trajectory-dependent first passage time, τ_i, which is defined as the time at which $\beta(\tau_i) = 1$ for the first time in the i-th trajectory (Figure 6c). The values of $\Delta t/\tau_i$ of the three trajectories shown are 0.16, 0.016, and 0.02, respectively, which is a reflection of the dynamic cooperativity of the locking process.

The number of water molecules, $N_W(t)$, in the vicinity of $G^1NNQQNY^7$ averaged over time in steps $\Delta = 1$ ns, was examined (14). As the locking reaction progresses, water molecules in the vicinity of the monomer in the fibril that are closest to the solvated monomer (the first β-strand shown in silver in Figure 6) are expelled. The coincidence of the locking step and dehydration is also reflected in the sharp, almost step-wise, decrease in the water content in the zipper region of the Sup35 crystal (Figure 6c). The number of water molecules, $N_W^Z(t)$, decreases abruptly, from eight to two, as the docking is initiated, and finally goes to

zero, as the locking process is complete (Figure 6c). These observations demonstrate that dehydration, resulting in the formation of the dry zipper region (13) as the monomer locks into the fibril lattice, is a key event in the growth of the amyloid fibrils. It is reasonable to surmise that interactions involving water must play an important role in the fibril growth (14, 99, 100).

6. MOVING FORWARD: SECRETASES AND CLEAVAGE OF APP

The primary component of AD-related amyloid plaques is the Aβ-peptide, a 38-to-43 amino acid polypeptide of known sequence (75, 101). Aβ-protein is produced from APP, a type I transmembrane (TM) glycoprotein in neural and non-neural cells. The cleavage of APP resulting in Aβ-peptide is achieved through the action of specific proteases termed secretases (102). APP is first cleaved at the β-site (forming the N terminus of Aβ-protein) by β-secretase, and the extracellular domain of APP is dissociated from the remaining protein (APP-C99). γ-secretase then cleaves the γ-site (Gly38-Thr43), which is located on the TM domain of APP-C99, and Aβ-protein is released to the extracellular region (103, 104). Because the γ-site contains several cleavage points (see Figure 7), Aβ of different chain lengths are observed. Of these, $A\beta_{1-40}$ and $A\beta_{1-42}$ are primary and secondary isoforms, respectively.

Many of the familial AD-associated mutations occur close to the secretase cleavage sites (Figure 7). Furthermore, it is known that variations in APP sequence correlate with the overall level of production of $A\beta$-protein and the distribution of $A\beta$-protein isoforms. An important focus of current research on AD is to understand the elementary steps in the process of cleavage of APP by γ-secretase and how that cleavage is influenced by APP sequence as well as environmental factors. As γ-secretase plays an important role in the process of essential proteins such as Notch, the inhibition of γ-secretase is not a viable therapeutic approach to the treatment of AD. However, the modulation of the activity of γ-secretase in cleaving APP, through the binding of small-molecule γ-secretase modulators to APP, is a potentially fruitful approach that is currently being explored (106, 107).

To address the process of Aβ-protein production and provide a structural basis for drug targets, researchers developed a computational model to examine the role of APP sequence on the structure of the critical TM helix of APP-C99. It has been postulated that the helix stability in the critical peptide region near the γ-cleavage site may provide information on how sequence can influence the point of cleavage, distribution of resulting Aβ-protein isoforms, and the overall level of Aβ-protein production (102).

6.1. Modeling the Structural Ensemble of APP-C99 in a Membrane Environment

A computational model of the TM helical region of the APP-C99 protein was developed and used to explore the nature of the APP-C99 structural ensemble in a membrane environment (108). The APP-C99 protein was modeled using its first 55 residues, APP fragment 672–726 referred to as $A\beta_{1-55}$. The protein was modeled in an implicit membrane environment based on the GBSW model (109–111) and the CHARMM22 force field (112). The membrane was 35 Å thick with a 5-Å membrane/solvent interfacial distance. Sampling was performed

using replica exchange molecular dynamics (REMD) (113) with 32 replicas ranging from 300 K to 700 K and 320 ns of dynamics. The average secondary structure of the protein at 300 K was analyzed using the DSSP (define secondary structure of proteins) algorithm (114) and the weighted histogram analysis method (115).

The simulation results for the secondary structure of $A\beta_{1-55}$ at 300 K are shown in Figure 8 along with the population of domains and sites of $A\beta_{1-55}$ at 300 K projected onto the z axis, which is normal to the solvent-membrane interface. The structures depicted are representative of the ensemble of $A\beta_{1-55}$ peptide structures occupying the global minimum of the free energy landscape.

The structure of $A\beta_{1-55}$ in the membrane has one long TM helix (30–35) that consists of domain B and C, and a small helical domain A (13–18). The secondary structure observed in our simulations of $A\beta_{1-55}$ is similar to that of APP-C99 in the LMPG micelle, proposed by NMR spectroscopy (116). The TM helix bends around Gly_{37} and Gly_{38}, and domain B (30–35) displays significant fluctuations. The peptide residues between Leu_{34} and Leu_{52} are found in the hydrophobic core region of the membrane (see Figure 8b). Lys and Gly residues play important roles in determining the nature of the peptide membrane interaction. Both residues can be located at the interface. The residues Lys_{28}, Gly_{29}, Gly_{37}, and Gly_{38} of $A\beta_{1-40}$ were found to be localized at the interface between the hydrophobic core region and lipid head group region in the membrane. Lys_{28}, Gly_{29}, Gly_{33}, Lys_{53}, Lys_{54}, and Lys_{55} of $A\beta_{1-55}$ are located near the interface between the membrane and the solvent. As a result, the Lys residues serve as anchors located at the opposing interfaces.

The simulation studies of the early stages of APP processing and Aβ-protein production provide insight into the role of sequence and environment in controlling the level of amyloid protein production and the distribution of amyloid protein isoforms believed to be critical to the evolution of Aβ-protein aggregation in vivo. The resulting observations led to important conjectures regarding how sequence may determine the stability of the critical TM helix of APP containing the γ-cleavage site, the angle of peptide insertion in a membrane, and the propensity of helix dimerization, considerations that are essential aspects of Aβ-peptide production in the initial stages of the aggregation pathway (117, 118).

6.2. Sequence Effects and Stability of APP-C99 Dimer Formation in a Membrane Environment

In a subsequent study, REMD simulations of two 33-residue proteins, APP fragments 694–726 referred to as $A\beta_{23-55}$, were performed in an implicit membrane environment for both the WT sequence and a mutant, in which Gly29 and Gly33 were replaced with Leu29 and Leu33 to probe how conformational differences between the WT and the mutant affect the cleavage of APP by γ-secretase and the resulting distribution of Aβ-peptides (119).

The effects of solvent and membrane on the APP fragments were included implicitly using the CHARMM force field with the EEF solvation model (112, 120). The REMD simulations allowed large movements of the APP fragment dimer in the membrane, without trapping any local minimum conformations. As depicted in Figure 9, dimerization of the WT results from

the two CαH…O hydrogen bonds between two APP-C99 fragments, whereas dimerization of the mutant results from hydrophobic interactions. In the mutant, each APP fragment is more tilted, and the γ-cleavage site is shifted toward the center of the membrane producing a mismatch between the active site of γ-secretase and the γ-cleavage site of APP that might prohibit Aβ production.

Three different types of homodimer conformations of APP-C99 fragments in the membrane environment were observed. (*a*) Dimers of WT protein were observed to be stabilized by C_α – H…O hydrogen bonds between the two APP-C99 fragments. These bonds are the most characteristic interaction between two fragments that contain Gly-XXX-Gly motifs (117). Owing to the three Gly-XXX-Gly motifs in the WT APP fragments, multiple C_α – H…O hydrogen bonds were observed. Of these, the hydrogen bonds involving Gly33 and Gly38 were essential for the dimerization of the WT APP fragments. (*b*) Dimers were also observed to be stabilized by interpeptide contacts between hydrophobic residues of the two APP-C99 fragments. This conformation was observed mainly in the mutant in which Leu29 and Leu33 contributed significantly to its stability. (*c*) A final dimer structure was observed to consist of two APP fragments crossed at Gly38 and forming a conformation similar to that of glycophorin A, which also contains a Gly-XXX-Gly motif in the TM region.

Our simulations indicate that the γ-site (Gly38-Thr43) in the mutant is shifted downward approximately 3 Å along the bilayer normal. In addition, the conformational flexibility of the γ-site is increased in the mutant as a result of the lack of interpeptide C_α – H…O hydrogen bonds at Gly38. These results suggest that the structural changes induce mismatched interactions between the γ-site of APP-C99 and the active site of γ-secretase, which would reduce the secretion of $A\beta_{1-40}$ or $A\beta_{1-42}$ as observed in experiment (117).

7. CONCLUSIONS AND PERSPECTIVES

Significant advances in the use of experiment to probe protein aggregation have led to the determination of high-resolution structures and reliable structural models for amyloid fibrils (121), placement of discrete mobile water molecules in amyloid fibrils (122), growth kinetics of oligomers, and energetics of fibril formation. Simultaneously, the past decade has witnessed increasing activity using theoretical and computational approaches, which have led to a coherent framework for describing the complex conformational transitions that drive fibril formation.

Despite significant progress, there remain a number of outstanding problems of biological and biophysical interest that will surely captivate our imaginations for years to come. Integration of experiments and computations will be necessary to make optimal progress in the vital areas of research identified here. Although the link between biophysical studies and attempts to understand the molecular basis of AD and other neurodegenerative diseases is not straightforward, it is clear that the concepts developed using theory and computations will have a significant impact in describing the molecular basis of protein aggregation.

Below we provide a brief summary of our current understanding and a prejudiced list of problems that we feel are perfectly suited for study at this time, using a variety of computational approaches described in this perspective.

ACKNOWLEDGMENTS

We are grateful to Leigh Foster, Francesca Massi, Naoyuki Miyashita, Edward O'Brien, Yuko Okamoto, Govardhan Reddy, Eva Rivera, Yuji Sugita, and Bogdan Tarus for collaborations and discussions. We thank Govardhan Reddy for composing Figures 2 and 6. Our work on protein aggregation has been generously supported by NIH for a number of years (R01 GM076688).

LITERATURE CITED

1. Dobson CM. 1999. Protein misfolding, evolution and disease. Trends Biochem. Sci 24:329–32 [PubMed: 10470028]
2. Chiti F, Dobson CM. 2006. Protein misfolding, functional amyloid, and human disease. Annu. Rev. Biochem 75:333–66 [PubMed: 16756495]
3. Bucciantini M, Giannoni E, Chiti F, Baroni F, Formigli L, et al. 2002. Inherent toxicity of aggregates implies a common mechanism for protein misfolding diseases. Nature 416:507–11 [PubMed: 11932737]
4. Dobson CM. 2006. The generic nature of protein folding and misfolding. Protein Rev 4:21–41
5. Maji SK, Perrin MH, Sawaya MR, Jessberger S, Vadodaria K, et al. 2009. Functional amyloids as natural storage of peptide hormones in pituitary secretory granules. Sciemce 325:328–32
6. Aguzzi A 2009. Cell biology: beyond the prion principle. Nature 459:924–25 [PubMed: 19536253]
7. Fowler DM, Kelly JW. 2009. Aggregating knowledge about prions and amyloid. Cell 137:20–22 [PubMed: 19345180]
8. Auer S, Dobson CM, Vendruscolo M, Maritan A. 2008. Self-templated nucleation in peptide and protein aggregation. Phys. Rev. Lett 101:258101–4 [PubMed: 19113754]
9. Prusiner SB. 1998. Prions. Proc. Natl. Acad. Sci. USA 95:13363–83 [PubMed: 9811807]
10. Lansbury PT Jr. 1996. A reductionist view of Alzheimer's disease. Acc. Chem. Res 29:317–21
11. Teplow DB, Lazo ND, Bitan G, Bernstein S, Wyttenbach T, et al. 2006. Elucidating amyloid-β protein folding and assembly: a multidisciplinary approach. Acc. Chem. Res 39:635–45 [PubMed: 16981680]
12. Straub JE, Thirumalai D. 2010. Principles governing oligomer formation in amyloidogenic peptides. Curr. Opin. Struct. Biol 20:187–95 [PubMed: 20106655]
13. Nelson R, Sawaya MR, Balbirnie M, Madsen AO, Riekel C, et al. 2005. Structure of the cross-β spine of amyloid-like fibrils. Nature 435:773–78 [PubMed: 15944695]
14. Reddy G, Straub JE, Thirumalai D. 2009. Dynamics of locking of peptides onto growing amyloid fibrils. Proc. Natl. Acad. Sci. USA 106:11948–53 [PubMed: 19581575]
15. Maggio JE, Mantyh PW. 1996. Brain amyloid: a physicochemical perspective. Brain Pathol 6:147–62 [PubMed: 8737930]
16. Teplow DB. 1998. Structural and kinetic features of amyloid β-protein fibrillogenesis. Amyloid 5:121–42 [PubMed: 9686307]
17. Thirumalai D, Klimov DK, Dima RI. 2003. Emerging ideas on the molecular basis of protein and peptide aggregation. Curr. Opin. Struct. Biol 13:146–59 [PubMed: 12727507]
18. Lomakin A, Chung DS, Benedek GB, Kirscher DA, Teplow DB. 1996. On the nucleation and growth of amyloid β-protein fibrils: detection of nuclei and quantitation of rate constants. Proc. Natl. Acad. Sci. USA 93:1125–29 [PubMed: 8577726]
19. Lomakin A, Teplow DB, Kirschner DA, Bendek GB. 1997. Kinetic theory of fibrillogenesis of amyloid β-protein. Proc. Natl. Acad. Sci. USA 94:7942–47 [PubMed: 9223292]
20. Eigen M 1996. Prionics or the kinetic basis for prion diseases. Biophys. Chem 63:A1–18 [PubMed: 8981746]

21. Kusumoto Y, Lomakin A, Teplow DB, Bendek GB. 1998. Temperature dependence of amyloid β-protein fibrillization. Proc. Natl. Acad. Sci. USA 95:12277–82 [PubMed: 9770477]
22. Palitto MM, Murphy RM. 2001. A mathematical model of the kinetics of β-amyloid fibril growth from the denatured state. Biophys 7. 81:1805–22
23. Hall D, Hirota N, Dobson CM. 2005. A toy model for predicting the rate of amyloid formation from unfolded protein. 7. Mol. Biol 195:195–205
24. Kim JR, Murphy RM. 2004. Mechanism of accelerated assembly of β-amyloid filaments into fibrils by $KLVFFK_6$. Biophys 7. 86:3194–203
25. Kim JR, Muresan A, Lee KYC, Murphy RM. 2004. Urea modulation of β-amyloid fibril growth: experimental studies and kinetic models. Prot. Sci 13:2888–98
26. Gibson TJ, Murphy RM. 2005. Design of peptidyl compounds that affect β-amyloid aggregation: importance of surface tension and context. Biochemistry 44:8898–907 [PubMed: 15952797]
27. Liu L, Murphy RM. 2006. Kinetics of inhibition of β-amyloid aggregation by transthyretin. Biochemistry 45:15702–9 [PubMed: 17176092]
28. Klimov DK, Straub JE, Thirumalai D. 2004. Aqueous urea solution destabilizes $A\beta_{16–22}$ oligomers. Proc. Natl. Acad. Sci. USA 101:14760–65 [PubMed: 15465917]
29. Knowles TPJ, Waudby CA, Devlin GL, Cohen SIA, Aguzzi A, et al. 2009. An analytical solution to the kinetics of breakable filament assembly. Science 326:1533–37 [PubMed: 20007899]
30. Harper JD, Wong SS, Lieber CM, Lansbury PT Jr. 1997. Observation of metastable Aβ amyloid protofibrils by atomic force microscopy. Chem. Biol 4:119–25 [PubMed: 9190286]
31. Walsh DM, Lomakin A, Bendek GB, Condron MM, Teplow DB. 1997. Amyloid β-protein fibrillogenesis: detection of a protofibrillar intermediate.J. Biol. Chem 272:22364–72 [PubMed: 9268388]
32. Harper JD, Wong SS, Lieber CM, Lansbury PT Jr. 1997. Atomic force microscopic imaging of seeded fibril formation and fibril branching by the Alzheimer's disease amyloid- β protein. Chem. Biol 4:951–59 [PubMed: 9427660]
33. Esler WP, Stimson ER, Ghilardi JR, Vinters HV, Lee JP, et al. 1996. In vitro growth of Alzheimer's disease β-amyloid plaques displays first-order kinetics. Biochemistry 35:749–57 [PubMed: 8547255]
34. Massi F, Straub JE. 2001. Energy landscape theory for Alzheimer's amyloid β-peptide fibril elongation. Proteins 42:217–29 [PubMed: 11119646]
35. Buell AK, Blundell JR, Dobson CM, Welland ME, Trentjev EM, Knowles TPJ. 2010. Frequency factors in a landscape model of filamentous protein aggregation. Phys. Rev. Lett 104:228101 [PubMed: 20873942]
36. Lee CF, Loken J, Jean L, Vaux DJ. 2009. Elongation dynamics of amyloid fibrils: a rugged energy landscape picture. Phys. Rev. E 80:041906
37. Esler WP, Stimson ER, Jennings JM, Vinters VH, Ghilardi JR, et al. 2000. Alzheimer's disease amyloid propagation by a template-dependent dock-lock mechanism. Biochemistry 39:6288–95 [PubMed: 10828941]
38. Jang H, Hall CK, Zhou Y. 2004. Assembly and kinetic folding pathways of a tetrameric beta-sheet complex: molecular dynamics simulations on simplified off-lattice protein models. Biophys. J 86:31–49 [PubMed: 14695247]
39. Jang H, Hall CK, Zhou Y. 2004. Thermodynamics and stability of a beta-sheet complex: molecular dynamics simulations on simplified off-lattice protein models. Prot. Sci 13:40–53
40. Peng S, Ding F, Urbanc B, Buldyrev SV, Cruz LC, et al. 2004. Discrete molecular dynamics simulations of peptide aggregation. Phys. Rev. E 69:041908–14
41. Borreguero JM, Ding F, Buldyrev SV, Stanley HE, Dokholyan NV. 2004. Multiple folding pathways of the SH3 domain. Biophys. J 87:521–33 [PubMed: 15240485]
42. Cruz L, Urbanc B, Borreguero JM, Lazo ND, Teplow DB, Stanley HE. 2005. Solvent and mutation effects on the nucleation of amyloid β-protein folding. Proc. Natl. Acad. Sci. USA 102:18258–63 [PubMed: 16339896]
43. Pellarin R, Caflisch A. 2006. Interpreting the aggregation kinetics of amyloid peptides. J. Mol. Biol 360:882–92 [PubMed: 16797587]

44. Derreumaux P, Mousseau N. 2007. Coarse-grained protein molecular dynamics simulations. J. Chem. Phys 126:025101 [PubMed: 17228975]
45. Bellesia G, Shea J-E. 2009. Diversity of kinetic pathways in amyloid fibril formation. J. Chem. Phys 131:111102 [PubMed: 19778093]
46. Pellarin R, Guarnera E, Caflisch A. 2007. Pathways and intermediates of amyloid fibril formation. J. Mol. Biol 374:917–24 [PubMed: 18028943]
47. Bellesia G, Shea J-E. 2009. Effect of β-sheet propensity on peptide aggregation. J. Chem. Phys 130:145103 [PubMed: 19368476]
48. Bellesia G, Shea J-E. 2007. Self-assembly of β-sheet forming peptides into chiral brillar aggregates. J. Chem. Phys 126:245104 [PubMed: 17614592]
49. Peterson JM, Fixman M. 1963. Viscosity of polymer solutions. J. Chem. Pbys 39:2516–23
50. Massi F, Peng JW, Lee JP, Straub JE. 2001. Simulation study of the structure and dynamics of the Alzheimer's amyloid peptide congener in solution. Biophys. J 80:31–44 [PubMed: 11159381]
51. Klimov DK, Thirumalai D. 2003. Dissecting the assembly of Aβ16–22 amyloid peptides into antiparallel β-sheets. Structure 11:295–307 [PubMed: 12623017]
52. Hills RD Jr, Brooks CL III. 2007. Hydrophobic cooperativity as a mechanism for amyloid nucleation. J. Mol. Biol 368:894–901 [PubMed: 17368485]
53. Fink AL. 1998. Protein aggregation: folding aggregates, inclusion bodies and amyloid. Fold. Des 3:R9–23 [PubMed: 9502314]
54. Kelly JW. 1998. The alternative conformations of amyloidogenic proteins and their multi-step assembly pathways. Curr. Opin. Struct. Biol 8:101–6 [PubMed: 9519302]
55. Hammarström P, Wiseman RL, Powers ET, Kelly JW. 2003. Prevention of transthyretin amyloid disease by changing protein misfolding energetics. Science 299:713–16 [PubMed: 12560553]
56. Dima RI, Thirumalai D. 2002. Exploring the propensities of helices in PrP^C to form β sheet using NMR structures and sequence alignments. Biophys. J 83:1268–80 [PubMed: 12202354]
57. Dima RI, Thirumalai D. 2004. Probing the instabilities in the dynamics of helical fragments from mouse PrP^C. Proc. Natl. Acad. Sci. USA 101:15335–40 [PubMed: 15494440]
58. Bae S-H, Legname G, Serban A, Prusiner SB, Wright PE, Dyson HJ. 2009. Prion proteins with pathogenic and protective mutations show similar structure and dynamics. Biochemistry 48:8120–28 [PubMed: 19618915]
59. Reddy AS, Wang L, Lin YS, Ling Y, Chopra M, et al. 2010. Solution structures of rat amylin peptide: simulation, theory, and experiment. Biophys. J 98:443–51 [PubMed: 20141758]
60. Urbanc B, Borreguero JM, Cruz L, Stanley HE. 2006. Amyloid β-protein aggregation: ab initio discrete molecular dynamics approach. Methods Enzymol 412:314–38 [PubMed: 17046666]
61. Mousseau N, Derreumaux P. 2008. Exploring energy landscapes of protein folding and aggregation. Front. Biosci 13:4495–516 [PubMed: 18508525]
62. Li MS, Klimov DK, Straub JE, Thirumalai D. 2008. Probing the mechanisms of fibril formation using lattice models. J. Chem. Phys 129:175101 [PubMed: 19045373]
63. Dill KA, Bromberg S, Yue KZ, Fiebig KM, Yee DP, et al. 1995. Principles of protein folding: a perspective from simple exact models. Prot. Sci 4:561–602
64. Dima RI, Thirumalai D. 2002. Exploring protein aggregation and self-propagation using lattice models: phase diagram and kinetics. Prot. Sci 11:1036–49
65. Gupta P, Hall CK. 1998. Effect of denaturant and protein concentration upon protein refolding and aggregation: a simple lattice model. Protein Sci 7:2642–52 [PubMed: 9865959]
66. Palyanov A, Krivov S, Karplus M, Chekmarev S. 2007. A lattice protein with an amyloidgenic latent state: stability and folding kinetics. J. Phys. Chem. B 111:2675–87 [PubMed: 17315918]
67. Straub JE, Thirumalai D. 1993. Exploring the energy landscape in proteins. Proc. Natl. Acad. Sci. USA 90:809–13 [PubMed: 8430090]
68. Straub JE, Rashkin A, Thirumalai D. 1994. Dynamics in rugged energy landscapes with applications to the s-peptide and ribonuclease a. J. Am. Chem. Soc 116:2049–63
69. Berne BJ, Straub JE. 1997. Novel methods of sampling phase space in the simulation of biological systems. Curr. Opin. Struct. Biol 7:181–89 [PubMed: 9094324]

70. Cheon M, Favrin G, Chang I, Dobson CM, Vendruscolo M. 2008. Calculation of the free energy barriers in the oligomerisation of Aβ peptide fragments. Front. Biosci 13:5614–22 [PubMed: 18508610]
71. Hardy J, Selkoe DJ. 2002. The amyloid hypothesis of Alzheimer's disease: progress and problems on the road to therapeutics. Science 297:353–56 [PubMed: 12130773]
72. Selkoe DJ. 1991. Alzheimer's disease: a central role for amyloid. J. Neuropathol 53:438–47
73. Cutler NR, Gottfries CG, Siegfried K. 1995. Alzheimer's Disease: Clinical and Treatment Perspectives West Sussex, UK: Wiley & Sons
74. Selkoe DJ. 1995. Deciphering Alzheimer's disease: Molecular genetics and cell biology yield major clues. J. NIH Res 7:57–64
75. Glenner GG, Wong CW. 1984. Alzheimer's disease: initial report of the purification and characterization of a novel cerebrovascular amyloid protein. Biochem. Biophys. Res. Commun 120:885–90 [PubMed: 6375662]
76. Masters CL, Simms G, Weinman NA, Multhaup G, McDonald BL, Beyreuther K. 1985. Amyloid plaque core protein in Alzheimer disease and Down syndrome. Proc. Natl. Acad. Sci. USA 82:4245–49 [PubMed: 3159021]
77. Lee JP, Stimson ER, Ghilardi JR, Mantyh PW, Lu YA, et al. 1995. ^{1}H NMR of Aβ amyloid peptide congeners in water solution: Conformational changes correlate with plaque competence. Biochemistry 34:5191–200 [PubMed: 7711039]
78. Esler WP, Stimson EV, Ghilardi JR, Lu Y, Felix A, et al. 1996. Point substitution in the central hydrophobic cluster of human β-amyloid congener disrupts peptide folding and abolishes plaque competence. Biochemistry 35:13914–21 [PubMed: 8909288]
79. Esler WP, Stimson ER, Lachenmann MJ, Ghilardi JR, Lu Y, et al. 2000. Activation barriers to structural transition determine deposition rates of Alzheimer's disease. J. Struct. Biol 130:174–83 [PubMed: 10940224]
80. Selkoe DJ. 2003. Folding proteins in fatal ways. Nature 426:900–4 [PubMed: 14685251]
81. Nguyen PH, Li MS, Stock G, Straub JE, Thirumalai D. 2007. Monomer adds to preformed structured oligomers of Aß-peptides by a two-stage dock-lock mechanism. Proc. Natl. Acad. Sci. USA 104:111–16 [PubMed: 17190811]
82. Takeda T, Klimov DK. 2009. Replica exchange simulations of the thermodynamics of Aβ fibril growth. Biophys. J 96:442–52 [PubMed: 19167295]
83. O'Brien EP, Okamoto Y, Straub JE, Brooks BR, Thirumalai D. 2009. Thermodynamic perspective on the dock-lock growth mechanism of amyloid fibrils. J. Phys. Chem. B 113:14421–30 [PubMed: 19813700]
84. Takeda T, Klimov DK. 2009. Side chain interactions can impede amyloid fibril growth: replica exchange simulations of Aβ peptide mutant. J. Phys. Chem. B 113:11848–57 [PubMed: 19708712]
85. Cannon MJ, Williams AD, Wetzel R, Myszka DG. 2004. Kinetic analysis of β-amyloid fibril elongation. Anal. Biochem 328:67–75 [PubMed: 15081909]
86. Petkova AT, Yau WM, Tycko R. 2006. Experimental constraints on quaternary structure in Alzheimer's β-amyloid fibrils. Biochemistry 45:498–512 [PubMed: 16401079]
87. Petkova AT, Leapman RD, Guo ZH, Yau WM, Mattson MP, Tycko R. 2005. Self-propagating, molecular-level polymorphism in Alzheimer's β-amyloid fibrils. Science 307:262–65 [PubMed: 15653506]
88. Tarus B, Straub JE, Thirumalai D. 2006. Dynamics of Asp23-Lys28 salt-bridge formation in Aβ 10–35 monomers. J. Am. Chem. Soc 128:16159–68 [PubMed: 17165769]
89. Tarus B, Straub JE, Thirumalai D. 2005. Probing the initial stage of aggregation of the $A\beta_{10-35}$ protein: assessing the propensity for peptide dimerization. J. Mol. Biol 345:1141–56 [PubMed: 15644211]
90. Baumketner A, Shea J-E. 2007. The structure of the Alzheimer amyloid-β (10–35) peptide probed through replica exchange molecular dynamics simulations in explicit solvent. J. Mol. Biol 366:275–85 [PubMed: 17166516]

91. Krone MG, Baumketner A, Bernstein SL, Wyttenbach T, Lazo NL, et al. 2008. Effects of familial Alzheimer's disease mutations on the folding nucleation of the amyloid β-protein. J. Mol. Biol 381:221–28 [PubMed: 18597778]
92. Murray MM, Krone MG, Bernstein SL, Baumketner A, Condron MM, et al. 2009. Amyloid β-protein: experiment and theory on the 21–30 fragment.J. Phys. Chem. B 113:6041–46 [PubMed: 19341254]
93. Tarus B, Straub JE, Thirumalai D. 2008. Structures and free-energy landscapes of the wild type and mutants of the Aβ (21–30) peptide are determined by an interplay between intrapeptide electrostatic and hydrophobic interactions. J. Mol. Biol 379:815–29 [PubMed: 18479708]
94. Straub JE, Guevara J, Huo SH, Lee JP. 2002. Long time dynamic simulations: exploring the folding pathways of an Alzheimer's amyloid Aβ peptide. Acc. Chem. Res 35:473–81 [PubMed: 12069633]
95. Melquiond A, Dong X, Mousseau N, Derreumaux P. 2008. Role of region 23–28 in Aβ fibril formation: insights from simulation of the monomers and dimers of Alzheimer's peptides Aβ 40 and Aβ 42. Curr. Alzheimer's Res 5:244–50
96. Baumketner A, Krone MG, Shea J-E. 2008. Role of the familial Dutch mutation E22Q in the folding and aggregation of the 15–28 fragment of the Alzheimer amyloid-β protein. Proc. Natl. Acad. Sci. USA 105:6027–32 [PubMed: 18408165]
97. Sciarretta KL, Gordon DJ, Petkova AT, Tycko R, Meredith SC. 2005. Aß 40-lactam(D23/K28) models a conformation highly favorable for nucleation of amyloid. Biochemistry 44:6003–14 [PubMed: 15835889]
98. Reddy G, Straub JE, Thirumalai D. 2009. Influence of preformed Asp23-Lys28 salt bridge on the conformational fluctuations of monomers and dimers of Aβ peptides with implications for rates of fibril formation. J. Phys. Chem. B 113:1162–72 [PubMed: 19125574]
99. Krone M, Hua L, Soto P, Zhou R, Berne B, Shea J-E. 2008. Role of water in mediating the assembly of Alzheimer amyloid-β Aβ (16–22) protofilaments. J. Am. Chem. Soc 120:11066–72
100. Reddy G, Straub JE, Thirumalai D. 2010. Dry amyloid fibril assembly in a yeast prion peptide is mediated by long-lived structures containing water wires. Proc. Natl. Acad. Sci. USA 107:21459–64 [PubMed: 21098298]
101. Roher AE, Ball MJ, Bhave SV, Wakade AR. 1991. β-Amyloid from Alzheimer disease brains inhibits sprouting and survival of sympathetic neurons. Biochem. Biophys. Res. Commun 174:572–79 [PubMed: 1993054]
102. Wolfe MS, Guénette SY. 2007. APP at a glance. J. Cell. Sci 120:3157–61 [PubMed: 17878232]
103. Wolfe MS. 2006. The γ-secretase complex: membrane-embedded proteolytic ensemble. Biochemistry 45:7931–39 [PubMed: 16800619]
104. Czirr E, Cottrell BA, Leuchtenberger S, Kukar T, Ladd TB, et al. 2008. Independent generation of Aβ42 and Aβ38 peptide species by γ-secretase. J. Biol. Chem 283:17049–54 [PubMed: 18426795]
105. Weksler ME, Gouras G, Relkin NR, Szabo P. 2005. The immune system, amyloid-β peptide, and Alzheimer's disease. Immunol. Rev 205:244–56 [PubMed: 15882358]
106. Kukar T, Golde TE. 2008. Possible mechanisms of action of NSAIDs and related compounds that modulate γ-secretase cleavage. Curr. Top. Med. Chem 8:47–53 [PubMed: 18220932]
107. Kukar TL, Ladd TB, Bann MA, Fraering PC, Narlawar R, et al. 2008. Substrate-targeting γ-secretase modulators. Nature 453:925–29 [PubMed: 18548070]
108. Miyashita N, Straub JE, Thirumalai D. 2009. Structures of β-amyloid peptide 1–40, 1–42, and 1–55—the 672–726 fragment of APP—in a membrane environment with implications for interactions with γ-secretase. J. Am. Chem. Soc 131:17843–52 [PubMed: 19995075]
109. Im W, Feig M, Brooks CL III. 2003. An implicit membrane generalized Born theory for the study of structure, stability, and interactions of membrane proteins. Biophys. J 85:2900–18 [PubMed: 14581194]
110. Im W, Lee MS, Brooks CL III. 2003. Generalized Born model with a simple smoothing function. J. Comp. Chem 24:1691–702 [PubMed: 12964188]
111. Feig M, Im W, Brooks CL III. 2004. Implicit solvation based on generalized Born theory in different dielectric environments. J. Chem. Phys 120:903–11 [PubMed: 15267926]

112. Mackerell AD Jr, Bashford D, Bellott M, Dunbrack RL Jr, Evanseck JD, et al. 1998. All-atom empirical potential for molecular modeling and dynamics studies of proteins. J. Phys. Chem. B 102:3586–616 [PubMed: 24889800]
113. Sugita Y, Okamoto Y. 1999. Replica-exchange molecular dynamics method for protein folding. Chem. Phys. Lett 314:141–51
114. Kabsch W, Sander C. 1983. Dictionary of protein secondary structure: pattern recognition of hydrogen-bonded and geometrical features. Biopolymers 22:2577–637 [PubMed: 6667333]
115. Kumar S, Rosenberg JM, Bouzida D, Swendsen RH, Kollman PA. 1992. The weighted histogram analysis method for free-energy calculations on biomolecules. I. The method. J. Comp. Chem 13:1011–21
116. Beel AJ, Mobley CK, Kim HJ, Tian F, Hadziselimovic A, et al. 2008. Structural studies of the transmembrane C-terminal domain of the amyloid precursor protein (APP): Does APP function as a cholesterol sensor? Biochemistry 47:9428–46 [PubMed: 18702528]
117. Kienlen-Campard P, Tasiaux B, Van Hees J, Li M, Huysseune S, et al. 2008. Amyloidogenic processing but not AICD production requires a precisely oriented APP dimer assembled by transmembrane GXXXG motifs. J. Biol. Chem 283:7733–44 [PubMed: 18201969]
118. Sato T, Tang T-C, Reubins G, Fei JZ, Fujimoto T, et al. 2009. A helix-to-coil transition at the ε-cut site in the transmembrane dimer of the amyloid precursor protein is required for proteolysis. Proc. Natl. Acad. Sci. USA 106:1421–26 [PubMed: 19164538]
119. Miyashita N, Straub JE, Thirumalai D, Sugita Y. 2009. Transmembrane structures of amyloid precursor protein dimer predicted by replica-exchange molecular dynamics simulations. J. Am. Chem. Soc 131:3438–39 [PubMed: 19275251]
120. Lazaridis T, Karplus M. 1999. Effective energy function for proteins in solution. Proteins 35:133–52 [PubMed: 10223287]
121. Balbach JJ, Ishii Y, Antzutkin ON, Leapman RD, Rizzo NW, et al. 2000. Amyloid fibril formation by $A\beta_{16-22}$, a seven-residue fragment of the Alzheimer's β-amyloid peptide, and structural characterization by solid state NMR. Biochemistry 39:13748–59 [PubMed: 11076514]
122. Kim YS, Liu L, Axelsen PH, Hochstrasser RM. 2009.2D IR provides evidence for mobile water molecules in β-amyloid fibrils. Proc. Natl. Acad. Sci. USA 106:17751–56 [PubMed: 19815514]
123. Goldschmidt L, Teng PK, Riek R, Eisenberg D. 2010. Identifying the amylome, proteins capable of forming amyloid-like fibrils. Proc. Natl. Acad. Sci. USA 107:3487–92 [PubMed: 20133726]

SUMMARY POINTS

1. The structures of amyloid fibrils are similar regardless of the sequence identity or the structure of the associating peptides or proteins. An implication is that there are a few aggregation mechanisms, which can be characterized by visualizing the cascade of events, that drive monomeric peptides to oligomers and eventually to fibrils, in terms of the complex energy landscape. In all scenarios, it is postulated that aggregation is facilitated by populating an ensemble of N^* structures, which can be quite distinct from the lowest free energy conformations adopted by the monomer.
2. Predictions for the rates of fibril growth kinetics as a function of monomer concentration can be made by picturing the monomer addition as a diffusive process in the amyloid energy landscape. The theory predicts a nonmonotonic variation in the equilibrium flux of fibril growth, as the monomer concentration changes, reflecting the underlying complex growth kinetics.
3. From a molecular perspective, formation of oligomers and fibrils occurs globally by a nearly universal two-stage dock-lock mechanism. In the first dock stage, a monomer adds on to a preexisting fibril by a diffusion-limited process. In the second stage, the monomer undergoes substantial conformational rearrangement to lock into a structure defined by the amyloid fibril. The two-stage growth mechanism is illustrated using lattice models and all-atom simulations of Aβ-peptides.
4. In the early stages of oligomer formation in Aβ-peptides, a discrete set of water molecules is expelled. The resulting oligomer resembles a fluctuating soluble nematic droplet with a dry interface between the peptides forming the interior. In the late stages of fibril growth in peptides from yeast prion, drying occurs cooperatively and abruptly in two stages. Water expulsion and locking of the peptide coincide in the second stage.
5. Studies of the structural ensemble of APP in a membrane environment may provide insights into the processing of APP by secretases to form Aβ-peptides. The development of a clear structural basis for production of $A\beta_{1-40}$ and $A\beta_{1-42}$, in terms of the interaction between specific sites on APP and γ-secretase, may inform efforts to devise appropriate ligands for controlling the cleavage products.

FUTURE ISSUES

1. The viewpoint that the ensemble of N^* structures triggers association implies that the morphology of the fibrils may be discernible by exhaustively enumerating the folding landscape of the monomer. Is it possible that variations in the packing of different N^* structures underlie the observed polymorphism of the fibrils? If not, at what stage of the growth process can the emergence of polymorphism be identified?

2. Can the regions prone to conformational changes during the aggregation process be identified using sequence information alone? Our perspective is that sequence and structural information must be combined at least through knowledge of the N^* ensemble, including knowledge of excitations around the low free energy monomer structures, to predict the potential structures that emerge as the aggregation reaction proceeds. Recently, it has been suggested (123) that searching for sequence motifs that pack into a steric zipper, as found in the fibrils from the C-terminal heptapeptide from yeast prions, can be a harbinger of amyloidogenic tendencies. Does this conclusion remain valid when aggregation in full-length proteins is considered?

3. The precise role water plays in facilitating amyloid fibril formation is a vexing problem that is sure to challenge experiments despite recent progress (122). Simulations of association of predominantly hydrophobic Aβ-peptide sequence (51, 99) and all-polar peptide from Sup35 (100) reveal drastically different roles for water. In the former cases, expulsion of water occurs rapidly. In the latter, long-lived metastable structures stabilized by perfectly ordered water wires mediate the formation of dry protofilaments (100). What are the distinct roles for water in protein aggregation, and is a discrete set of trapped water molecules another possible source of polymorphism in amyloid fibrils?

4. How can we link the structures of APP in the presence of membranes to the kinetics of Aβ production? Providing a structural basis for these events represents a new frontier in the use of simulations (119) and is fundamental to our understanding of the role of secretases in AD.

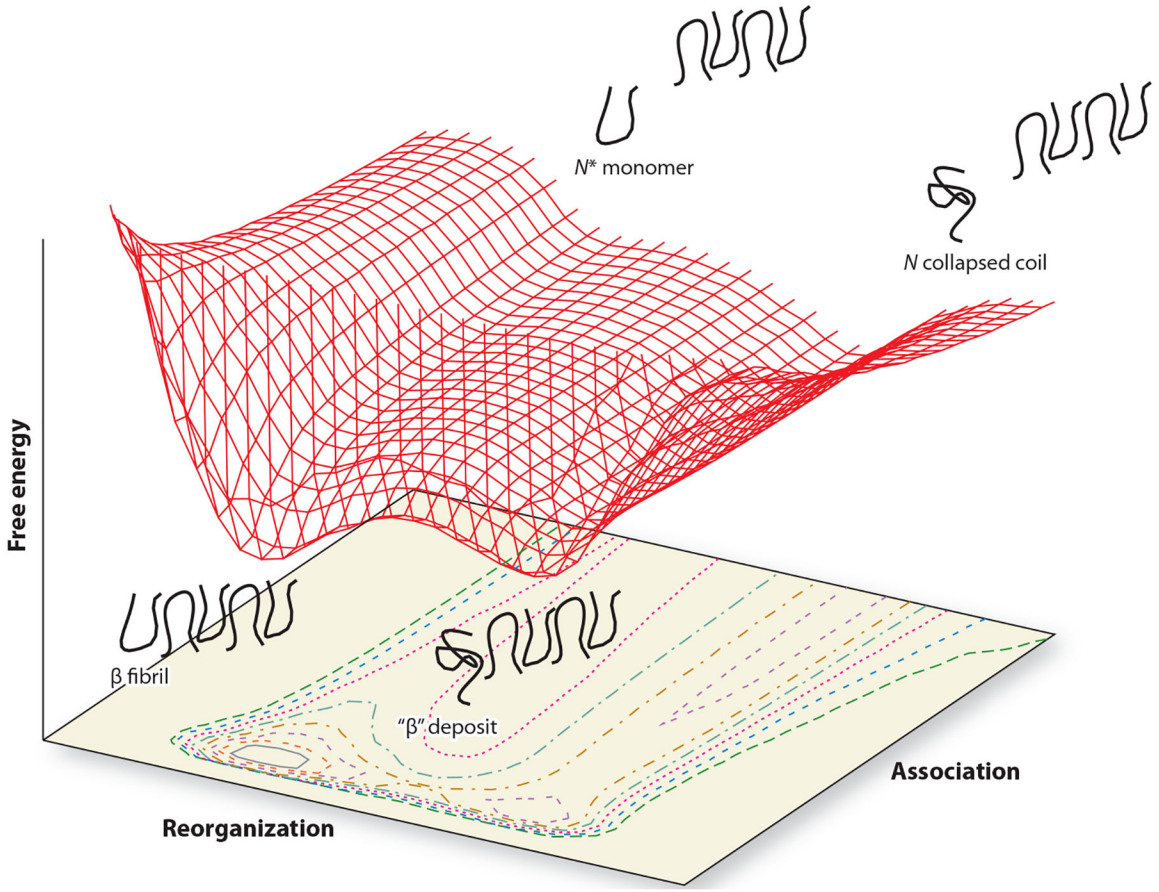

Figure 1.

Caricature of an energy landscape that captures essential features of the overall mechanism for amyloid peptide fibril elongation. Depicted on the energy surface are the thermodynamically stable peptide monomer in solution (N), the activated monomer in solution (N^*), the amorphous or poorly formed peptide/fibril deposit ("β "), and the well-formed peptide state (β). Figure adapted from Reference 34, figure 3.

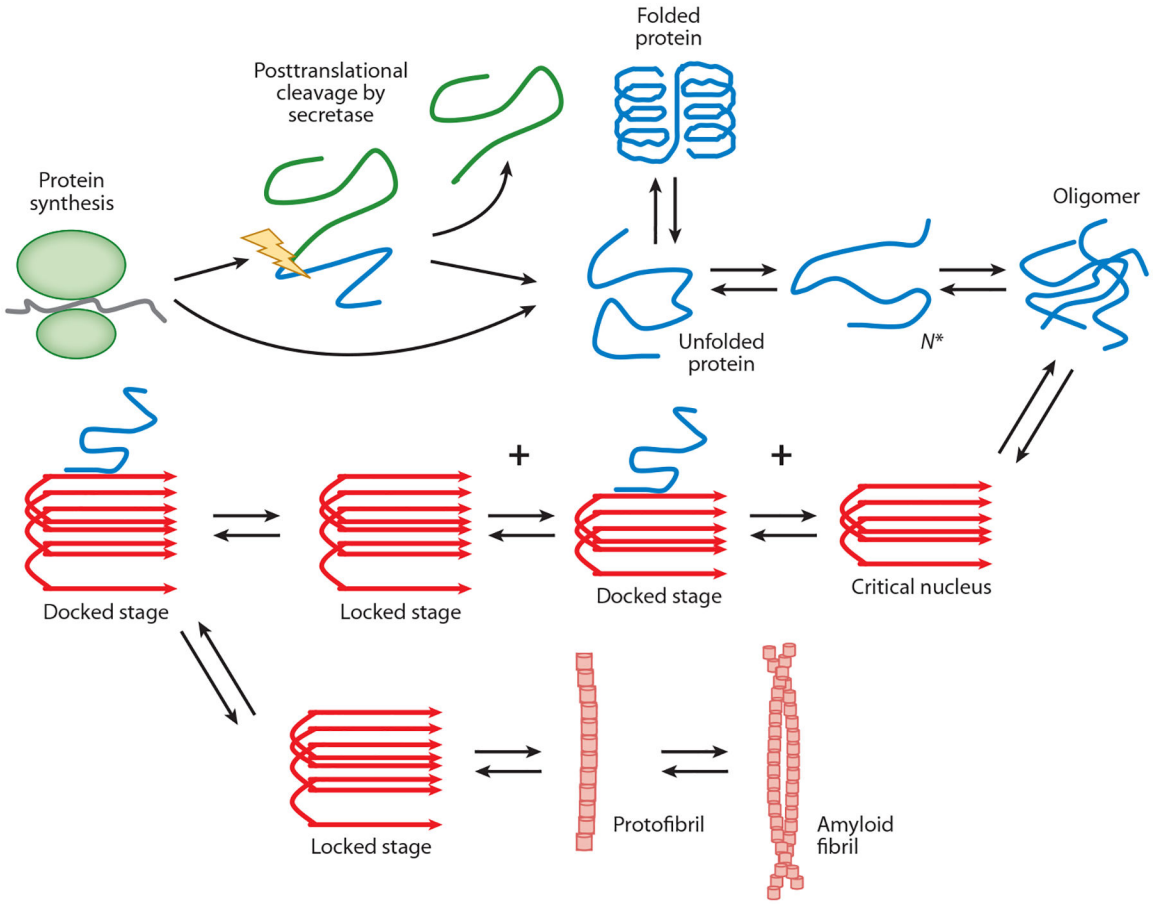

Figure 2.

Summary of kinetic steps in the formation of aggregation-prone states and fibrils from amyloid peptides. The key first step following the production of the amyloidogenic peptide is the formation of the aggregation-prone N^* (17).

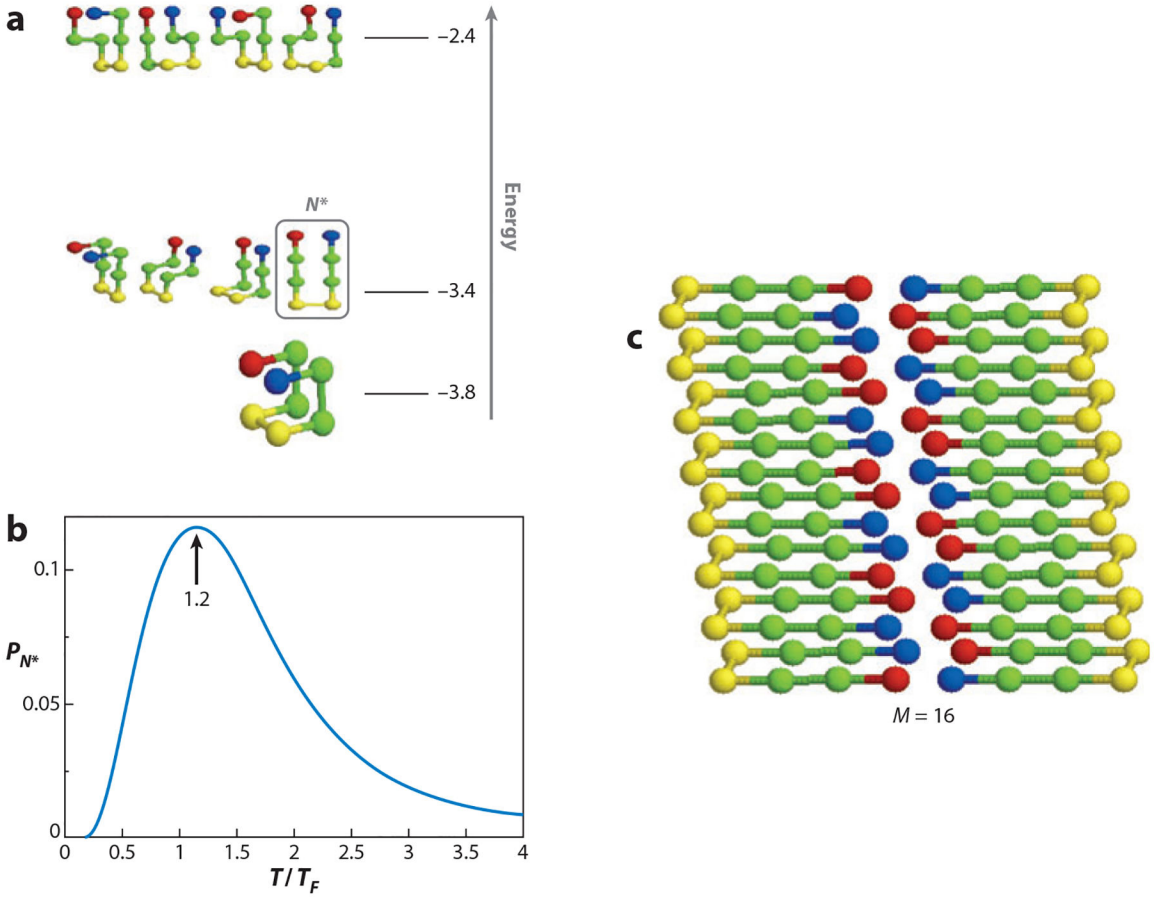

Figure 3.

The eight-bead lattice model: (*a*) spectrum of energy levels for peptide conformations and (*b*) probability of forming N^* as a function of temperature. (*c*) 16-mer lattice models appearing as an assembly of N^* configurations. Hydrophobic, polar, positively, and negatively charged beads are shown in green, yellow, blue, and red, respectively. Figure adapted from Reference 62, figures 1 and 2.

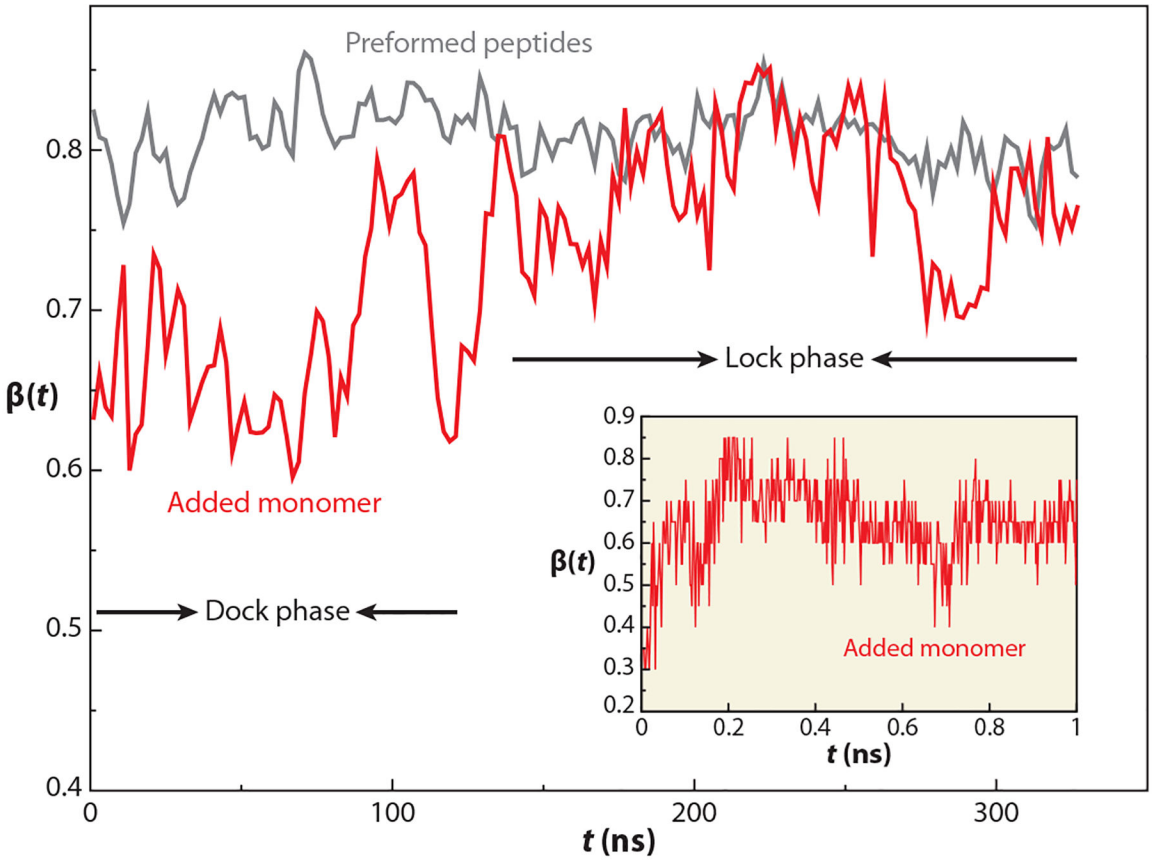

Figure 4.

Average time dependency of the β-strand content of the $A\beta_{16-22}$ peptide for the preformed pentamer and the added monomer and (*inset*) the trajectory-averaged strand content $\bar{\beta}(t)$. The value of $\beta(t)$ for the structured oligomer remains high and fluctuates around its initial value of roughly 0.8. The β-strand content of the added monomer is considerably less than that of the structured pentamer for $t < 120$ ns, which roughly corresponds to the dock phase. For $t > 120$ ns, which represents the lock phase, the β-strand content coincides with the value in the ordered state. Figure adapted from Reference 81, figure 5.

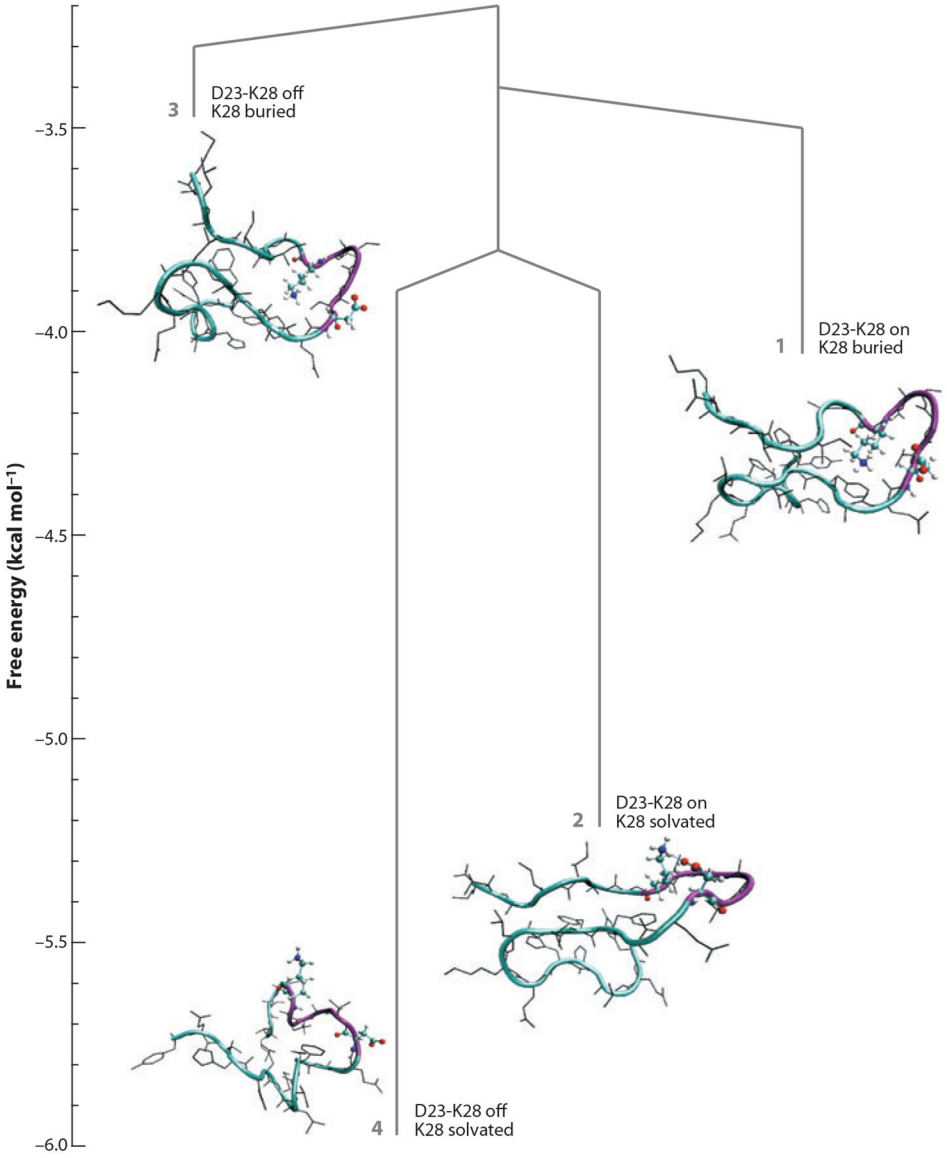

Figure 5.

Characterization of the free energy landscape of the $A\beta_{10-35}$ peptide, projected onto two key coordinates associated with salt-bridge formation, based on all-atom simulations in explicit aqueous solvent. Four superbasins are depicted as on (salt-bridge formed) and off (salt-bridge broken) states with conformations of K28 (solvated or buried). Figure adapted from Reference 88, figure 5.

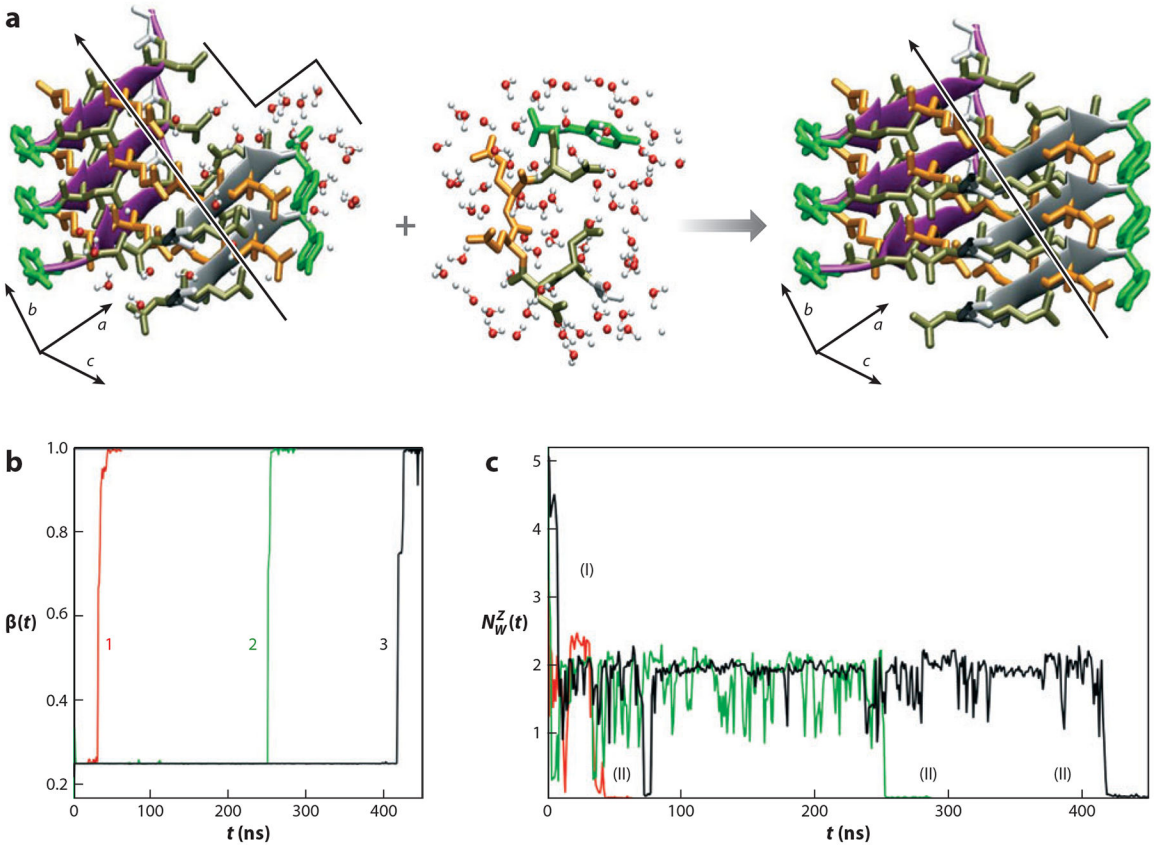

Figure 6.

(*a*) Pair of β-sheets from the Sup35 microcrystal. The arrow through the crystal is the fibril axis (the crystal orientation labeled as a, b, c is shown for clarity). One sheet is in purple and the other is shown in silver. The sheet in silver consists of two monomers creating a vacant position in the crystal. The missing monomer creates a terrace-like structure in the crystal at which the unstructured solvated monomer can associate, leading to fibril formation shown on the right (14). (*b*) Time-dependent changes in the β-strand content of the monomer, $\beta(t)$, during the locking process of the heptapeptide to the terrace junction. (*c*) Time-dependent changes in the number of water molecules in the zipper region. Water in the zipper region is expelled in two distinct stages. In stage I there are about seven to nine water molecules at the start of the lock phase, and the number decreases to about two in 10 ns. In stage II, water molecules are completely expelled as the monomer locks onto the fibril. The transitions in both stages are abrupt and reflect the increase in $\beta(t)$ in panel *b*. Figure adapted from Reference 14, figure 1.

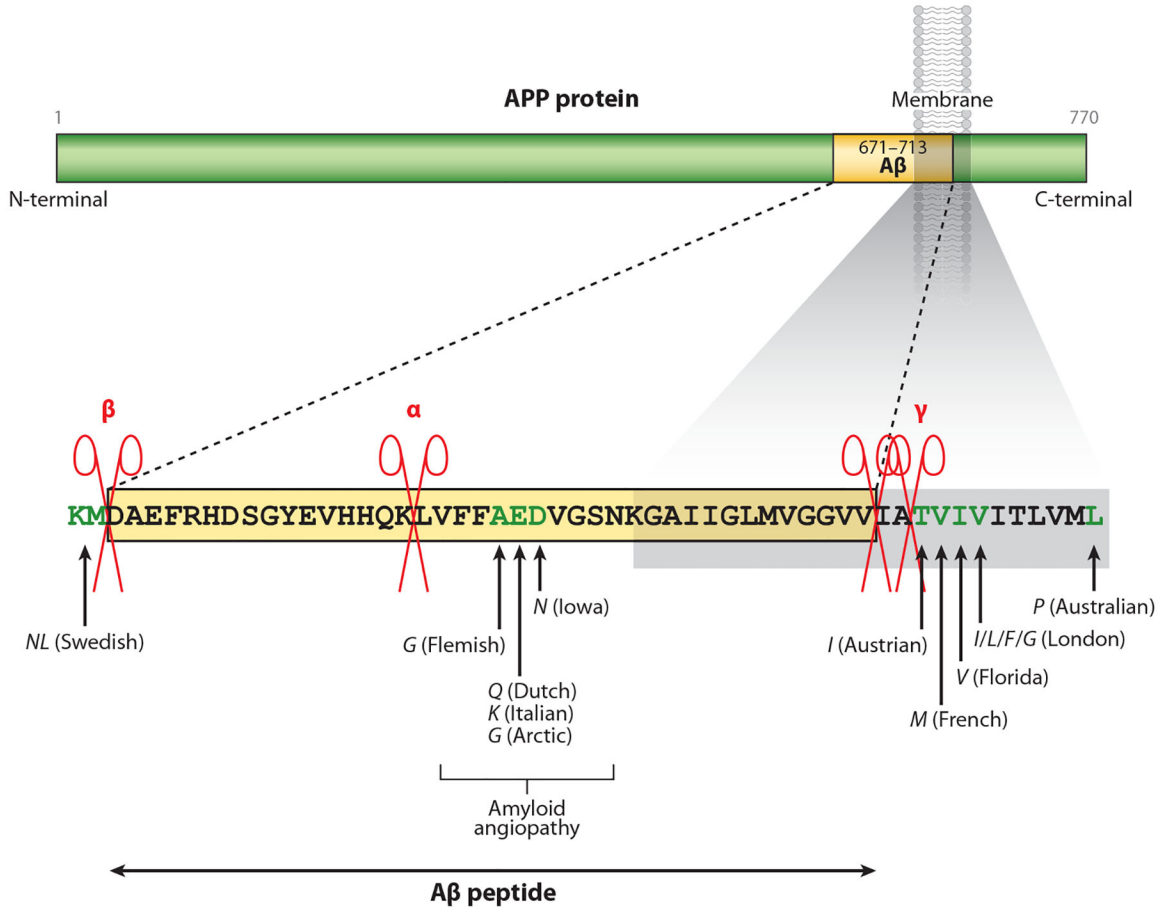

Figure 7.

Metabolic processing of amyloid precursor protein (APP) by secretases leads to Aβ-peptides of varying length. The cleavage sites for α-, β-, and γ-secretase are noted. Known familial mutations are clustered in regions of the APP sequence that correspond to the N- and C-terminal regions of the Aβ-protein. A third critical cluster of mutations is found on the N-terminal side of the VGSN turn region, a structural motif observed in the Aβ-protein in aqueous solution, membrane-mimicking solutions, micellular environments, and solid-state fibrils. Figure adapted from Reference 105, figure 2.

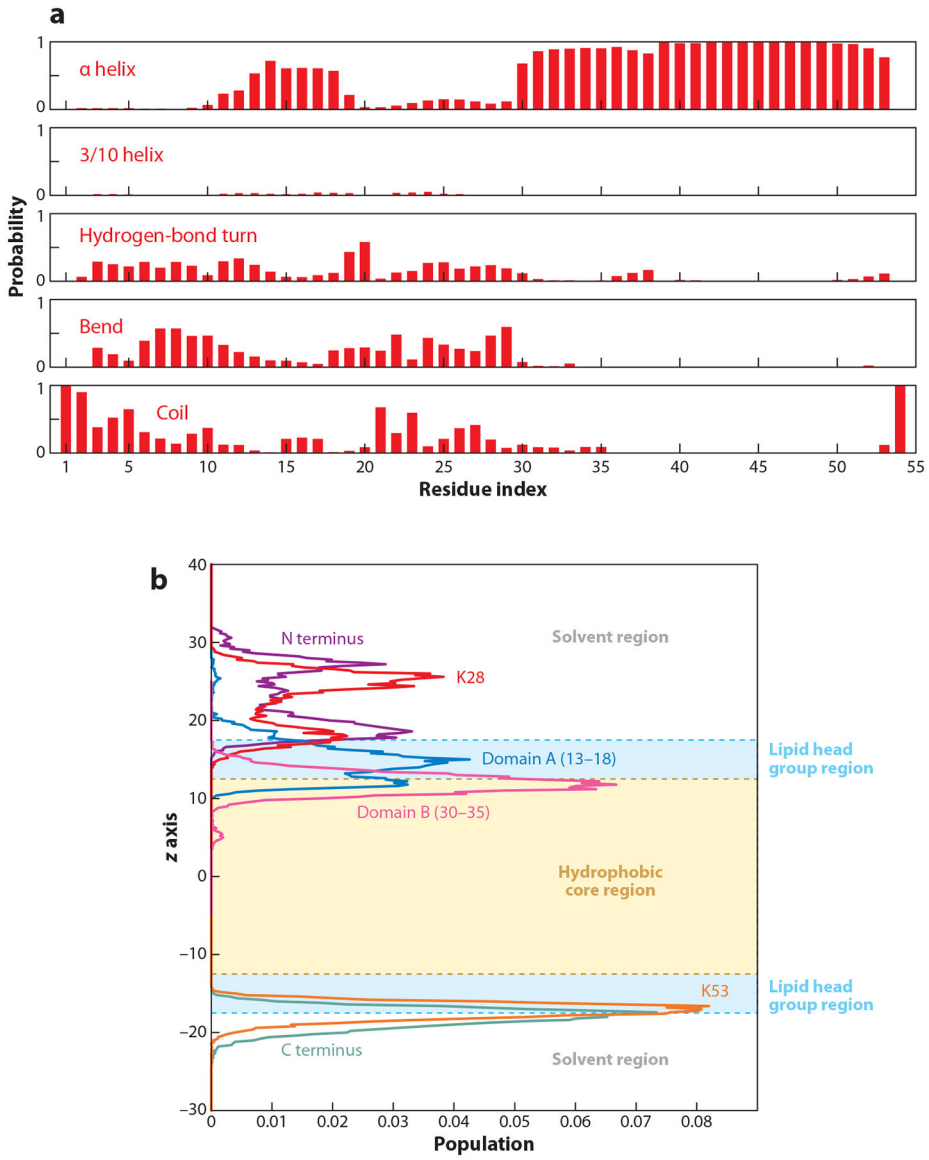

Figure 8.

Computed average $A\beta_{1-55}$ (*a*) secondary-structure probability, as a function of residue number, and (*b*) population of peptide domains projected along the normal direction to the membrane surface. The transmembrane helix is formed with high probability separated from a short α-helical region by a turn near the characteristic VGSN subsequence. Figure adapted from Reference 108, figure 5.

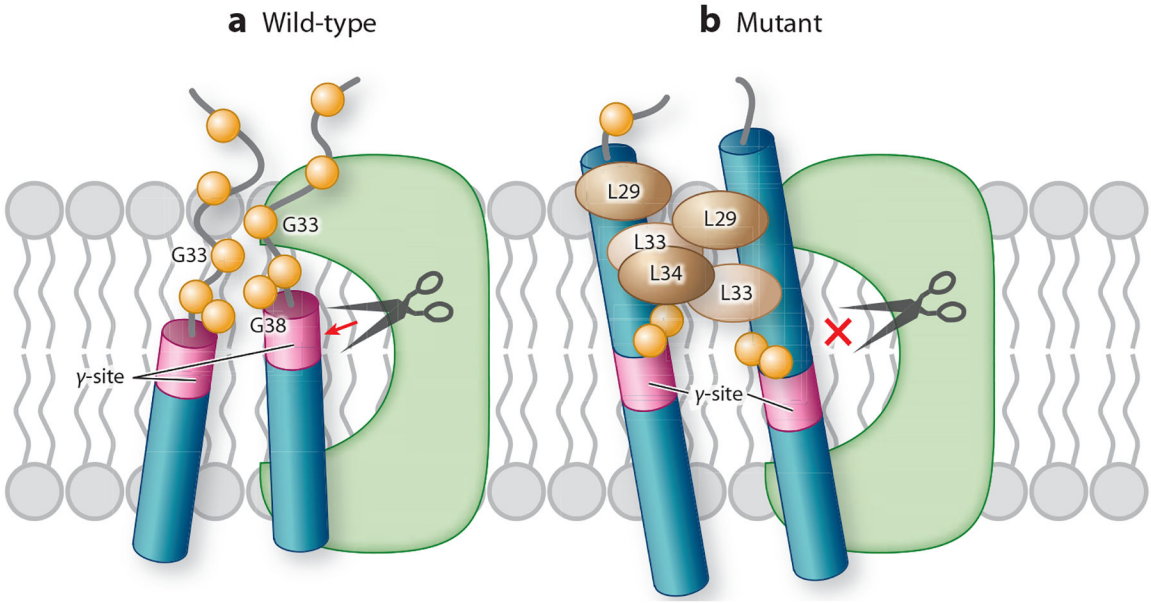

Figure 9.
A schematic illustration of the large conformational differences between the wild-type and the mutant amyloid precursor protein (APP) fragments in the membrane environment. Figure adapted from Reference 119.